Cellular/Molecular

Probing $\alpha_4\beta\delta$ $GABA_A$ Receptor Heterogeneity: Differential Regional Effects of a Functionally Selective $\alpha_4\beta_1\delta/\alpha_4\beta_3\delta$ Receptor Agonist on Tonic and Phasic Inhibition in Rat Brain

Kirsten Hoestgaard-Jensen, Nils Ole Dalby, Jacob Krall, Harriet Hammer, Povl Krogsgaard-Larsen, Bente Frølund, and Anders A. Jensen

Department of Drug Design and Pharmacology, Faculty of Health and Medical Sciences, University of Copenhagen, 2100 Copenhagen OE, Denmark

In the present study, the orthosteric $GABA_A$ receptor ($GABA_AR$) ligand 4,5,6,7-tetrahydroisothiazolo[5,4-*c*]pyridin-3-ol (Thio-THIP) was found to possess a highly interesting functional profile at recombinant human $GABA_ARs$ and native rat $GABA_ARs$. Whereas Thio-THIP displayed weak antagonist activity at $\alpha_{1,2,5}\beta_{2,3}\gamma_{2S}$ and ρ_1 $GABA_ARs$ and partial agonism at $\alpha_6\beta_{2,3}\delta$ $GABA_ARs$ expressed in *Xenopus* oocytes, the pronounced agonism exhibited by the compound at $\alpha_4\beta_1\delta$ and $\alpha_4\beta_3\delta$ $GABA_ARs$ was contrasted by its negligible activity at the $\alpha_4\beta_2\delta$ subtype. To elucidate to which extent this *in vitro* profile translated into functionality at native $GABA_ARs$, we assessed the effects of 100 μM Thio-THIP at synaptic and extrasynaptic receptors in principal cells of four different brain regions by slice electrophysiology. In concordance with its $\alpha_6\beta_{2,3}\delta$ agonism, Thio-THIP evoked robust currents through extrasynaptic $GABA_ARs$ in cerebellar granule cells. In contrast, the compound did not elicit significant currents in dentate gyrus granule cells or in striatal medium spiny neurons (MSNs), indicating predominant expression of extrasynaptic $\alpha_4\beta_2\delta$ receptors in these cells. Interestingly, Thio-THIP evoked differential degrees of currents in ventrobasal thalamus neurons, a diversity that could arise from differential expression of extrasynaptic $\alpha_4\beta\delta$ subtypes in the cells. Finally, whereas 100 μM Thio-THIP did not affect the synaptic currents in ventrobasal thalamus neurons or striatal MSNs, it reduced the current amplitudes recorded from dentate gyrus granule cells, most likely by targeting perisynaptic $\alpha_4\beta\delta$ receptors expressed at distal dendrites of these cells. Being the first published ligand capable of discriminating between β_2- and β_3-containing receptor subtypes, Thio-THIP could be a valuable tool in explorations of native $\alpha_4\beta\delta$ $GABA_ARs$.

Key words: **$\alpha4\beta\delta$; extrasynaptic; GABA; GABA-A receptors; subtype-selective; tonic inhibition**

Introduction

The fast signaling of the major inhibitory CNS neurotransmitter GABA is mediated by $GABA_A$ receptors ($GABA_ARs$), a family of pentameric anion-selective ligand-gated ion channels belonging to the Cys-loop receptor superfamily (Whiting, 2003; Olsen and Sieghart, 2008). Native $GABA_AR$ subtypes are assembled from a total of 19 subunits (α_1-α_6, β_1-β_3, γ_1-γ_3, δ, ε, π, θ, ρ_1-ρ_3), and the differential *in vivo* distribution of these subunits combined with the distinct functional properties of the assembled subtypes enable the receptors to mediate a wide range of functions throughout the CNS (Pirker et al., 2000; Olsen and Sieghart, 2008; Hörtnagl et al., 2013). The synaptic $GABA_ARs$ responsible for phasic inhibition are predominantly made up by α_1, α_2, and/or α_3 in combination with β_2/β_3 and γ_2 subunits, whereas the $\alpha_4\beta\delta$, $\alpha_6\beta\delta$, and $\alpha_5\beta\gamma_2$ subtypes constitute the major perisynaptic/extrasynaptic receptors mediating tonic inhibition of the GABAergic system (Whiting, 2003; Farrant and Nusser, 2005; Olsen and Sieghart, 2008; Belelli et al., 2009; Brickley and Mody, 2012). However, several additional physiologically relevant subtypes exist, and the distinction between synaptic and perisynaptic/extrasynaptic receptors is considerably less clear-cut than outlined above (Mortensen and Smart, 2006; Glykys et al., 2007; Eyre et al., 2012; Marowsky et al., 2012; Milenkovic et al., 2013).

Investigations into the physiological functions governed by different $GABA_AR$ subtypes have to a large extent relied on the use of subtype-selective ligands and/or knock-out or knock-in mice (Reynolds et al., 2003; Rudolph and Knoflach, 2011). The availability of allosteric modulators exhibiting functional selectivity for the different α-containing $\alpha_{1,2,3,5}\beta\gamma$ subtypes and of the agonist 4,5,6,7-tetrahydroisoxazolo[5,4-*c*]pyridin-3-ol (THIP) and positive allosteric modulators (PAMs) selective for the $\alpha_4\beta\delta/\alpha_6\beta\delta$ receptors has been instrumental for the explorations of

Received April 13, 2014; revised Oct. 14, 2014; accepted Oct. 20, 2014.

Author contributions: K.H.-J., N.O.D., and A.A.J. designed research; K.H.-J., N.O.D., H.H., and A.A.J. performed research; J.K., P.K.-L., and B.F. contributed unpublished reagents/analytic tools; K.H.-J., N.O.D., and A.A.J. analyzed data; A.A.J. wrote the paper.

This study was supported by the Novo Nordisk Foundation and the Lundbeck Foundation. We thank Drs. P.J. Whiting, D.S. Weiss, J. Clark, and B.R. Conklin for generous gifts of cDNAs; and Dr. H. Bräuner-Osborne for granting us access to the GAT-CHO cell lines.

The authors declare no competing financial interests.

Correspondence should be addressed to Dr. Anders A. Jensen, Department of Drug Design and Pharmacology, Faculty of Health and Medical Sciences, University of Copenhagen, Universitetsparken 2, 2100 Copenhagen OE, Denmark. E-mail: aaj@sund.ku.dk.

DOI:10.1523/JNEUROSCI.1495-14.2014

 0270-6474/14/3416256-17$15.00/0

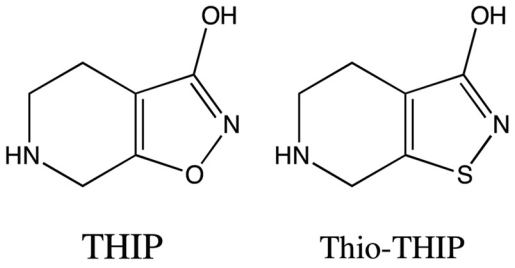

Figure 1. Chemical structures of THIP and Thio-THIP.

$GABA_A$Rs defined by their respective α subunits (Stórustovu and Ebert, 2006; Wafford et al., 2009; Hoestgaard-Jensen et al., 2010; Atack, 2011a, b). In contrast, the respective contributions of β_1-, β_2-, and β_3-containing receptors to GABAergic neurotransmission have not been delineated in similar detail, in no small part because of the limited number of β-isoform selective $GABA_A$R ligands available (Sieghart, 2006). Nevertheless, the differential CNS expression patterns of the three β subunits strongly suggest that different β-containing $GABA_A$R subtypes could mediate distinct physiological functions and that selective targeting of cross-sections of receptors other than those defined by α subunits could hold therapeutic potential.

The molecular composition of the orthosteric site located in the extracellular $\beta^{(+)}/\alpha^{(-)}$ interface of the pentameric $GABA_A$R complex is highly conserved throughout the receptors; thus, orthosteric ligands may not seem obvious candidates in the pursuit of subtype selectivity (Sieghart, 2006). Nonetheless, the functional subtype selectivity displayed by GABA analogs such as THIP and 5-(4-piperidyl)-3-isothiazolol (Thio-4-PIOL) underlines the feasibility of obtaining at least this form of selectivity through the site (Stórustovu and Ebert, 2006; Hoestgaard-Jensen et al., 2013). In the present study, the bicyclic 3-isothiazol GABA analog 4,5,6,7-tetrahydroisothiazolo[5,4-*c*]pyridin-3-ol (Thio-THIP) is demonstrated to possess a highly interesting functional profile at human $GABA_A$Rs expressed in *Xenopus* oocytes; and taking advantage of this functionality, Thio-THIP has been used to elucidate the heterogeneity of native $GABA_A$Rs in four rat brain regions.

Materials and Methods

Materials. Thio-THIP and THIP (Fig. 1) were synthesized in-house essentially as previously described (Krogsgaard-Larsen et al., 1977, 1983; Krehan et al., 2003). GABA, $ZnCl_2$, and chemicals used for buffers were purchased from Sigma-Aldrich, and SR95531 (gabazine) was obtained from Alamone Labs. DS2, picrotoxin, CGP 54626, and TTX were obtained from Tocris Bioscience Cookson, and Alexa-488-streptavidin was purchased from Invitrogen. *Xenopus laevis* oocytes and [^{3}H]GABA were obtained from Lohmann Research Equipment and PerkinElmer, respectively. The cDNAs encoding for the human $GABA_A$R subunits were kind gifts from Drs. P.J. Whiting and D.S. Weiss (ρ_1), whereas the cDNAs encoding for the rat $GABA_B$ receptors and the chimeric G-protein $G\alpha_{qi5}$ were kind gifts from Drs. J. Clark and B.R. Conklin, respectively.

Molecular biology. The subcloning of human α_1-α_5, β_2, γ_{2S}, and ρ_1 cDNAs into the pcDNA3.1 vector has been described previously (Jensen et al., 2010), and human β_3 cDNA in the pGEMHE vector was used in this study. The human α_6, β_1, and δ cDNAs were subcloned into pcDNA3.1 using the restriction enzyme pairs XhoI/XbaI (α_6 and δ) and NotI/XbaI (β_1). The cDNAs for chimeric subunits $\beta_2^{NTD}/\beta_3^{TMD/ICL}$ and $\beta_3^{NTD}/\beta_2^{TMD/ICL}$ were constructed using Splicing by Overlap Extension PCR (Horton et al., 1989) and subcloned into the pcDNA3.1 vector using the restriction enzymes NotI and XbaI. The $\beta_2^{NTD}/\beta_3^{TMD/ICL}$ and $\beta_3^{NTD}/\beta_2^{TMD/ICL}$ cDNAs encode for the mature proteins *Gln*^{1}-*Phe*^{212}|Arg^{213}-Asn^{448} and Gln^1-Phe^{212}|*Lys*^{213}-*Asn*^{450}, respectively (β_2 segments are given in italics). The integrity and the absence of unwanted mutations in all cDNAs created by PCR were verified by DNA sequencing (Eurofins MWG, Operon).

Ca^{2+}/Fluo-4 assay. The functional properties of Thio-THIP at $GABA_B$ receptors were characterized at rat $GABA_{B(1a,2)}$ and $GABA_{B(1b,2)}$ receptors coexpressed with the chimeric G-protein $G\alpha_{qi5}$ in tsA201 cells in the Ca^{2+}/Fluo-4 assay. The tsA201 cells were cultured in DMEM supplemented with 100 U/ml penicillin, 100 μg/ml streptomycin, and 10% fetal bovine serum. The 2×10^6 cells were split in a 10 cm tissue culture plate and transfected the following day with a total of 8 μg cDNA ($GABA_{B1a}$-pCDNA3.1 or $GABA_{B1b}$-pCDNA3.1, $GABA_{B2}$-pCDNA3.1 and $G\alpha_{qi5}$-pCDNAI in a 1:2:1 ratio) using Polyfect Transfection Reagent (QIAGEN). Sixteen to 24 h after transfection, the cells were split into poly-D-lysine-coated black 96-well plates with clear bottom. The following day, the culture medium was aspirated and the cells were incubated in 50 μl assay buffer (Hank's Buffered Saline Solution containing 20 mM HEPES, 1 mM $CaCl_2$, 1 mM $MgCl_2$, and 2.5 mM probenecid, pH 7.4) supplemented with 6 mM Fluo-4/AM (Invitrogen) at 37°C for 1 h. Then the buffer was aspirated, the cells were washed once with 100 μl assay buffer, and 100 μl assay buffer was added to the cells. The 96-well plate was then assayed in a NOVOstar microplate reader measuring emission (in fluorescence units) at 520 nm caused by excitation at 485 nm before and up to 60 s after addition of 33 μl agonist solution in assay buffer. The experiments were performed in duplicate three times for both GABA and Thio-THIP at both $GABA_B$ receptors.

[^{3}H]GABA uptake assay. The functional properties of Thio-THIP at GABA transporters were characterized at the human GAT-1, BGT-1, GAT-2, and GAT-3 subtypes stably expressed in Flp-In-CHO cells in a [^{3}H]GABA uptake assay essentially as previously described (Christiansen et al., 2008; Kvist et al., 2009). The cells were cultured in Ham's F-12 medium with L-glutamine supplemented with 100 U/ml penicillin, 100 μg/ml streptomycin, 10% FBS, 5 μg/ml plasmocin, and 200 μg/ml hygromycin B. Cells were split into poly-D-lysine-coated white 96-well plates; and the following day, the culture medium was removed and cells were washed with 100 μl assay buffer (Hank's Buffered Saline Solution containing 20 mM HEPES, 1 mM $CaCl_2$, and 1 mM $MgCl_2$, pH 7.4). Then 100 μl assay buffer supplemented with 100 nM [^{3}H]GABA and various concentrations of the test compounds was added onto the cells, and the plate was incubated at 37°C for 3 min. Then the cells were washed with 2×100 μl ice-cold assay buffer, and 150 μl Microscint20 scintillation fluid (PerkinElmer) was added to each well. The plate was shaken for at least 1 h, after which the radioactivity in the wells was counted in a Wallac 1450 MicroBeta Trilux scintillation counter (GMI). The experiments were performed in triplicate four times for both GABA and Thio-THIP at all four GABA transporters.

X. laevis *oocytes and two-electrode voltage clamp.* The $GABA_A$R subunit cDNAs were linearized, transcribed, and capped in using the mMessage mMachine T7 kit (Ambion). $\alpha_{1,2,5}\beta_{2,3}\gamma_{2S}$ cRNAs were mixed and injected into oocytes in a subunit ratio of 1:1:1 (concentration of each subunit: 10 ng/μl; injection volumes: 4–18 nl), whereas $\alpha_{4,6}\beta_{1,2,3}\delta$ cRNAs were mixed and injected in a subunit ratio of 10:1:10 (concentrations of subunits: 1 μg/μl (α), 0.1 μg/μl (β), and 1 μg/μl (δ); injection volume: 46 nl). As for the homomeric receptors, the ρ_1 cRNA (concentration: 0.1 μg/μl) was injected in a volume of 4–18 nl, whereas the respective β_1, β_2, and β_3 cRNAs (concentrations: 0.2 μg/μl) were injected in volumes of 32–46 nl. The oocytes were incubated for 1–7 d in modified Barth's saline (88 mM NaCl, 1 mM KCl, 15 mM HEPES, pH 7.5, 2.4 mM $NaHCO_3$, 0.41 mM $CaCl_2$, 0.82 mM $MgSO_4$, 0.3 mM $Ca(NO_3)_2$, 100 U/ml penicillin, and 100 μg/ml streptomycin). Oocytes were clamped at −40 mV to −90 mV with an Oocyte Clamp OC-725C amplifier (Warner), and both voltage and current electrodes were agar-plugged with 3 M KCl (resistances: 0.5–2.0 MΩ). In the agonist experiments, GABA, THIP, or Thio-THIP was applied to the perfusate until the peak of the response was observed. To avoid receptor desensitization, a washout period of 2.2 min was executed between drug applications. In the antagonist experiments, the oocyte was preincubated for 30 s with the test compound before coapplication of test compound and GABA. The incorporation of the γ_{2S} subunit into the receptors assembled at the cell surface of $\alpha_{1,2,5}\beta_{2,3}\gamma_{2S}$-expressing oocytes was confirmed

with 100 μM $ZnCl_2$ (Karim et al., 2013), and the presence of δ in cell surface-expressed $\alpha_4\beta\delta$ and $\alpha_6\beta\delta$ receptors was confirmed using the δ-$GABA_AR$ selective PAM DS2 (Wafford et al., 2009) and 1 μM $ZnCl_2$ (Stórustovu and Ebert, 2006). All oocyte data were based on recordings performed on oocytes from at least two different batches. The recorded baseline-to-peak current amplitudes were analyzed using Clampfit 10.1 (Molecular Devices) and normalized to the maximum current amplitude elicited by GABA at the individual oocyte. Data were analyzed and fitted to concentration–response or concentration–inhibition curves by use of the nonlinear regression in GraphPad Prism 5 (GraphPad Software), with the fittings of the biphasic and triphasic concentration–response curves for GABA and THIP at $\alpha_4\beta_1\delta$ and $\alpha_4\beta_3\delta$ being performed by eye.

Slice electrophysiology: animals. Young adult male Sprague Dawley rats from Harlan Laboratories, weighing 200–250 g at the time of experiment, were used for the preparation of acute brain slices. Animals were housed at a normal 12 h light/dark cycle at 22°C–25°C in cages of up to 6 rats. The protocols were approved by the Danish Authorities for Animal Experimentation.

Slice preparation. After decapitation, the brain was rapidly dissected out in ice-cold low-Na artificial CSF (NMDG-ACSF) containing the following (in mM): NaCl (26), *N*-methyl-D-glucamine-HCl (100), KCl (2.5), $CaCl_2$ (1), $MgCl_2$ (3), $NaHCO_3$ (26), NaH_2PO_4 (1.25), D-glucose (10), ascorbate (0.3), pyruvic acid (1.0), and kynurenic acid (2). The osmolality of NMDG-ACSF was adjusted to 310 ± 5 mOsm. The brain was glued to the platform of a Leica 1200 VS microtome and cut in ice-cold NMDG-ACSF. Orientation and slice thickness were as follows: striatum (coronal, 250 μm), hippocampus (horizontal, 350 μm), ventrobasal thalamus (coronal 250 μm), and cerebellum (sagittal, 250 μm). After cutting, slices were stored in regular ACSF, which differs from NMDG-ACSF by the omission of kynurenic acid and by NMDG-HCl being replaced by NaCl (total 126 mM NaCl) at 28°C for 1–4 h. All solutions were bubbled with carbogen (95% O_2/5% CO_2).

Whole-cell recordings. For recordings of the effects of Thio-THIP at $GABA_AR$s at synaptic and extrasynaptic loci, slices were maintained submerged in a 2 ml chamber perfused with ACSF at a flow of 2.5 ml/min at 33°C–34°C and included 2 mM kynurenic acid, 1 μM CGP 54626, and 1 μM TTX. Recordings that included $ZnCl_2$ (15 μM) were performed in phosphate-free ACSF. Cells were visualized using a custom-built infrared video-microscopy system. Somatic whole-cell recordings in voltage-clamp were made using a Multiclamp 700A amplifier (Axon Molecular Devices). Recordings were digitized at 10 kHz on a 1320 digidata digitizer (Axon Molecular Devices) and lowpass filtered (8-pole Bessel) at 3 kHz. The intracellular solution contained the following (in mM): CsCl (135), NaCl (4), $MgCl_2$ (2), EGTA (0.1), HEPES (10), ATP (2), GTP (0.5), TEA (5), and QX-314 (5), with pH adjusted to 7.3 (at 4°C) and osmolality to 292 mOsm. Patch pipettes were pulled with tip diameters required for neurons of the different regions and with resistance ranging from 5 MΩ (hippocampal granule cells) to 10–11 MΩ (cerebellar granule cells) using this solution. All cells were held at −70 mV for the duration of the experiment, and recordings were 70% compensated for series resistance and discarded for further analysis if values for capacitance and series resistance during recordings deviated >30% from initial values. After establishment of whole-cell configuration, cells were held for a minimum of 6 min to allow for perfusion of intracellular solution and stabilize holding current before recording of baseline (3 min) followed by drug perfusion (6 min). Recordings were stopped 1 min after addition of SR95531 directly to the bath resulting in a very fast rise in concentration to ~100 μM SR95531. A few cells from each region (except cerebellum) were recorded with the intracellular solution containing 1% biocytin for postrecording visualization of cellular architecture by the Alexa-488-coupled streptavidin system as previously described (Hoestgaard-Jensen et al., 2013).

Data analysis. All whole-cell recordings were made in pClamp 10 and further analyzed in either Clampfit 10 (Axon Molecular Devices) or for the spontaneous events, in Mini Analysis 6.03 (Synaptosoft) and Origin 9.0 (OriginLab). A two-sample *t* test with equal variance assumed and $p < 0.05$ as level of significance was used for assessment of drug effects in individual groups, and a one-way ANOVA ($p < 0.05$) with *post hoc* Bonferroni test to assess significance of differences in mean current density across cell types. For detection of mIPSCs, an algorithm in Mini Analysis 6.03 was made to detect baseline deflections of 5 × SD of the trace and sampling 5 ms before and 50 ms after detection. The threshold value for mIPSC detection was determined while drug was perfused. For construction of an average waveform of the synaptic current, events with an interevent interval <50 ms were removed, and the remaining non-contaminated events were aligned with respect to the 50% rising phase. The averaged synaptic current was characterized by the 20%–80% rise time (RT_{20-80}), peak, weight of tau, and area. The weight of tau, τ_w, was calculated from a fit to a biexponential using $\tau_w = (A1/(A1 + A2)) \times \tau_1 + (A2/(A1 + A2)) \times \tau_2$, in which A1/A2 and τ_1/τ_2 are the amplitudes and tau values of the individual exponentials. The current induced by THIP or Thio-THIP was measured as the difference in the holding current of two 30 s windows, the first located 30 s before compound entered the bath and the second immediately before addition of SR95531 to the bath. The holding current in the 30 s window was measured as the center of a Gaussian of 1 ms sampled baseline every 100 ms. The currents are reported relative to the capacitance of the recorded neuron (i.e., current density pA/pF), and data are given as means ± SEM.

Results

Functional characterization of Thio-THIP at recombinant human $GABA_AR$s

In a screening program in which a series of GABA analogs synthesized by the Krogsgaard-Larsen group over the years were tested at selected $GABA_AR$ subtypes, the compound Thio-THIP was found to exhibit an interesting functional profile (unpublished observations). Thio-THIP has previously been reported to exhibit ~300-fold lower binding affinity to native $GABA_AR$s in rat synaptosomes than the closely related analog THIP, to induce neuronal depression in cat spinal cord neurons, and to be a weak competitive antagonist at human $\alpha_3\beta_2\gamma_2$ and $\alpha_5\beta_3\gamma_2$ $GABA_AR$s expressed in *Xenopus* oocytes (Krogsgaard-Larsen et al., 1983; Brehm et al., 1997). Nevertheless, the findings in the screening prompted us to explore the pharmacology of Thio-THIP in further detail, and the functional properties displayed by the compound in two-electrode voltage-clamp recordings at 13 human $GABA_AR$ subtypes expressed in *Xenopus* oocytes will be presented below. Prior to this, however, the basic functional characteristics exhibiting the three $\alpha_4\beta\delta$ subtypes in this study will be outlined, since the functional properties exhibited by $\alpha_4\beta\delta$ $GABA_AR$s expressed in oocytes in previous studies have varied considerably. Thus, because of the key importance of these receptors for this study, their basic functional properties are important to consider when interpreting the findings for Thio-THIP.

Basic functional characteristics of $\alpha_4\beta\delta$ $GABA_AR$s expressed in *Xenopus* oocytes

In agreement with previous studies, GABA displayed distinct monophasic concentration–response curves at the $\alpha_1\beta_2\gamma_{2S}$, $\alpha_1\beta_3\gamma_{2S}$, $\alpha_2\beta_2\gamma_{2S}$, $\alpha_2\beta_3\gamma_{2S}$, $\alpha_5\beta_2\gamma_{2S}$, $\alpha_5\beta_3\gamma_{2S}$, $\alpha_6\beta_2\delta$, $\alpha_6\beta_3\delta$, and ρ_1 $GABA_AR$ subtypes expressed in oocytes (Table 1) (Mortensen et al., 2011; Hoestgaard-Jensen et al., 2013; Karim et al., 2013). Analogously, monophasic concentration–response curves were consistently observed for GABA at the $\alpha_4\beta_2\delta$ $GABA_AR$, whereas the concentration–response relationships exhibited by the agonist at the $\alpha_4\beta_1\delta$ and $\alpha_4\beta_3\delta$ receptors were considerably more complex. The GABA concentration–response curves at $\alpha_4\beta_3\delta$-expressing oocytes were consistently biphasic and characterized by mid-nanomolar and low-micromolar $EC_{50,1}$ and $EC_{50,2}$ values, respectively (Fig. 2*A*,*C*; Table 1). Because the relative sizes of the "high-affinity" and "low-affinity" components of the total response varied somewhat between the different oocytes, the bi-

Table 1. Functional properties of GABA, THIP, and Thio-THIP at human $GABA_ARs$ expressed in *Xenopus* oocytes[a]

	EC_{50} (pEC_{50} ± SEM)	n_H ± SEM	R_{max} ± SEM	*n*
GABA				
$\alpha_1\beta_2\gamma_{2S}$	38 (4.43 ± 0.09)	1.1 ± 0.05	100	5
$\alpha_1\beta_3\gamma_{2S}$	42 (4.38 ± 0.11)	0.9 ± 0.06	100	4
$\alpha_2\beta_2\gamma_{2S}$	46 (4.34 ± 0.08)	1.2 ± 0.12	100	4
$\alpha_2\beta_3\gamma_{2S}$	16 (4.80 ± 0.14)	1.1 ± 0.10	100	5
$\alpha_5\beta_2\gamma_{2S}$	42 (4.38 ± 0.05)	1.1 ± 0.06	100	5
$\alpha_5\beta_3\gamma_{2S}$	14 (4.85 ± 0.08)	1.1 ± 0.10	100	4
$\alpha_4\beta_1\delta$ (monophasic)	0.62 (6.20 ± 0.65)	0.4 ± 0.02	100	4
$\alpha_4\beta_1\delta$ (triphasic)	$EC_{50,1}$ ~0.17 (~6.8)	ND	(7 ± 2)[b]	
	$EC_{50,2}$ ~3.9 (~5.4)	ND	(65 ± 5)[b]	
	$EC_{50,3}$ ND	ND	100[c]	4
$\alpha_4\beta_2\delta$	2.5 (5.60 ± 0.20)	1.0 ± 0.09	100	4
$\alpha_4\beta_3\delta$ (biphasic)	$EC_{50,1}$ 0.011 (7.95 ± 0.15)	0.9 ± 0.17	(66 ± 7)[b]	
	$EC_{50,2}$ 3.2 (5.50 ± 0.15)	0.7 ± 0.13	100	8
$\alpha_4\beta_3$	0.31 (6.51 ± 0.01)	0.7 ± 0.07	100	3
$\alpha_6\beta_2\delta$	0.58 (6.24 ± 0.08)	0.9 ± 0.06	100	5
$\alpha_6\beta_3\delta$	0.87 (6.06 ± 0.15)	1.0 ± 0.05	100	5
ρ_1	1.8 (5.74 ± 0.05)	1.7 ± 0.40	100	4
$\alpha_4\beta_2^{NTD}/\beta_3^{TMD/ICL}\delta$	2.0 (5.70 ± 0.15)	0.9 ± 0.05	100	6
$\alpha_4\beta_3^{NTD}/\beta_2^{TMD/ICL}\delta$	1.1 (5.97 ± 0.08)	0.9 ± 0.08	100	5
THIP				
$\alpha_4\beta_1\delta$ (biphasic)	$EC_{50,1}$ ~0.14 (~6.9)	0.9 ± 0.13	(105 ± 31)[b]	
	$EC_{50,2}$ ND	ND	291 ± 3[c]	2
$\alpha_4\beta_1\delta$ (triphasic)	$EC_{50,1}$ ~0.32 (~6.5)	ND	(41 ± 2)[b]	
	$EC_{50,2}$ ~13 (~4.9)	ND	(135 ± 6)[b]	
	$EC_{50,3}$ ND	ND	312 ± 26[c]	7
$\alpha_4\beta_2\delta$	33 (4.48 ± 0.04)	0.7 ± 0.05	230 ± 9	4
$\alpha_4\beta_3\delta$	130 (3.90 ± 0.24)	0.7 ± 0.13	240 ± 12	4
Thio-THIP (agonist)				
$\alpha_5\beta_3\gamma_{2S}$	ND	ND	9 ± 1[c]	6
$\alpha_4\beta_1\delta$ (biphasic)	$EC_{50,1}$ ~1.0 (~6.0)	ND	(25 ± 5)[b]	
	$EC_{50,2}$ ND	ND	41 ± 1[c]	6
$\alpha_4\beta_2\delta$	ND	ND	4.3 ± 1[c]	7
$\alpha_4\beta_3\delta$	13 (4.89 ± 0.13)	0.61 ± 0.11	58 ± 7	9/25[e]
$\alpha_4\beta_3$	ND	ND	6.5 ± 2[c]	4
$\alpha_6\beta_2\delta$	~220 (~3.7)	ND	50 ± 8[d]	4
$\alpha_6\beta_3\delta$	~320 (~3.5)	ND	56 ± 11[d]	6
ρ_1	ND	ND	2 ± 3[c]	4
$\alpha_4\beta_2^{NTD}/\beta_3^{TMD/ICL}\delta$	ND	ND	14 ± 4[c]	7
$\alpha_4\beta_3^{NTD}/\beta_2^{TMD/ICL}\delta$	ND	ND	12 ± 3[c]	8
Thio-THIP (antagonist)				
$\alpha_1\beta_2\gamma_{2S}$	~300 (~3.5)[f]	—	—	3
$\alpha_1\beta_3\gamma_{2S}$	~400 (~3.4)[f]	—	—	8
$\alpha_2\beta_2\gamma_{2S}$	~300 (~3.5)[f]	—	—	4
$\alpha_2\beta_3\gamma_{2S}$	~800 (~3.1)[f]	—	—	3
$\alpha_5\beta_2\gamma_{2S}$	~600 (~3.2)[f]	—	—	6
$\alpha_4\beta_2\delta$	>1000 (<3.0)[f]	—	—	5
ρ_1	~150 (~3.8)[f]	—	—	4

[a]EC_{50} (in μM, with pEC_{50} values in parentheses), nH, and R_{max} (in % of the maximum response of GABA) values are given for the three agonists, and estimated IC_{50} values (in μM, with pIC_{50} in parentheses) are given for Thio-THIP at the receptors where it was tested as an antagonist (using GABA EC_{80} as agonist). The numbers of experiments performed (*n*) are also given. ND, Not determinable.

[b]Fitted maximal response for the phase (in % of R_{max} of GABA at the receptor).

[c]The concentration–response curve was not saturated at the highest agonist concentration tested. Thus, EC_{50} and n_H values could not be determined; and instead of the R_{max} value, the response elicited by the maximum agonist concentration used (1 mM THIP or 1 mM Thio-THIP) is given in % of R_{max} of GABA at the receptor.

[d]The concentration–response curve was not completely saturated at the highest agonist concentration tested. EC_{50} and R_{max} are estimated from the fitted curve.

[e]The averaged EC_{50} and n_H values for Thio-THIP are based on 9 complete concentration–response curves, whereas the averaged R_{max} value is based on 25 determinations.

[f]The concentration-inhibition curve was not completed at the highest Thio-THIP concentration tested. The IC_{50} value is estimated from the fitted curve.

phasic nature of the concentration–response curve is somewhat lost in the averaged data (Fig. 2*D*). Two divergent profiles were observed for GABA at $\alpha_4\beta_1\delta$ $GABA_AR$-expressing oocytes: a monophasic concentration–response curve (EC_{50} of 620 nM), and a multiphasic, possibly triphasic (see Materials and Methods) concentration–response curve with estimated $EC_{50,1}$ and $EC_{50,2}$ values of 170 nM and 3.9 μM and a third phase that did not reach saturation at GABA concentrations up to 10 mM (Fig. 2*A*,*C*; Table 1). In accordance with previous studies of the $\alpha_4\beta_3\delta$ $GABA_AR$ in oocytes (Stórustovu and Ebert, 2006; Meera et al., 2011), THIP was found to be a superagonist at all three $\alpha_4\beta\delta$ receptors, evoking twofold to threefold higher maximal re-

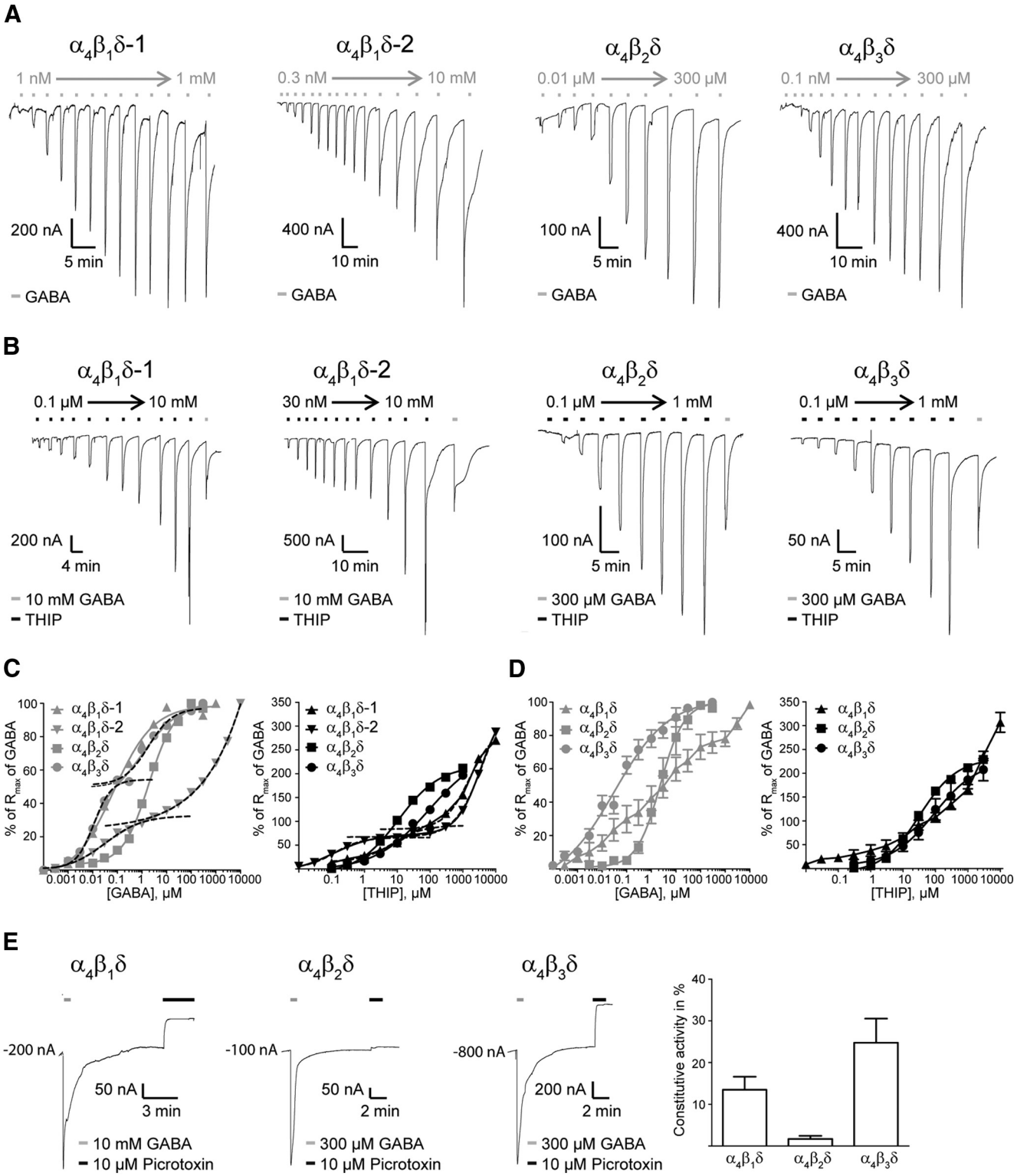

Figure 2. Basic functional characteristics of human $\alpha_4\beta\delta$ $GABA_ARs$ expressed in *Xenopus* oocytes. ***A***, Representative traces of the currents evoked by various concentrations of GABA at human $\alpha_4\beta_1\delta$, $\alpha_4\beta_2\delta$, and $\alpha_4\beta_3\delta$ $GABA_ARs$. The different profiles exhibited by GABA at $\alpha_4\beta_1\delta$ are exemplified as $\alpha_4\beta_1\delta$-1 and $\alpha_4\beta_1\delta$-2. ***B***, Representative traces of the currents evoked by various concentrations of THIP at human $\alpha_4\beta_1\delta$, $\alpha_4\beta_2\delta$, and $\alpha_4\beta_3\delta$ $GABA_ARs$. The different profiles exhibited by THIP at $\alpha_4\beta_1\delta$ are exemplified as $\alpha_4\beta_1\delta$-1 and $\alpha_4\beta_1\delta$-2. ***C***, Representative concentration–response curves for GABA and THIP at the $\alpha_4\beta_1\delta$, $\alpha_4\beta_2\delta$, and $\alpha_4\beta_3\delta$ $GABA_ARs$. The different profiles exhibited by GABA and THIP at the $\alpha_4\beta_1\delta$ $GABA_AR$ are given as $\alpha_4\beta_1\delta$-1 and $\alpha_4\beta_1\delta$-2. The curve fittings of the different phases of the GABA concentration–response relationships at $\alpha_4\beta_1\delta$-2 and $\alpha_4\beta_3\delta$ and of the THIP concentration–response relationships at $\alpha_4\beta_1\delta$-1 and $\alpha_4\beta_1\delta$-2 are given in hatched lines. ***D***, Averaged concentration–response curves for GABA and THIP at the $\alpha_4\beta_1\delta$, $\alpha_4\beta_2\delta$, and $\alpha_4\beta_3\delta$ $GABA_ARs$. Data are mean ± SEM (GABA: $n = 8$, $n = 4$, and $n = 9$ for $\alpha_4\beta_1\delta$, $\alpha_4\beta_2\delta$, and $\alpha_4\beta_3\delta$, respectively; THIP: $n = 9$, $n = 4$, and $n = 4$ for $\alpha_4\beta_1\delta$, $\alpha_4\beta_2\delta$, and $\alpha_4\beta_3\delta$, respectively). ***E***, Levels of constitutive activity in oocytes expressing human $\alpha_4\beta_1\delta$, $\alpha_4\beta_2\delta$, and $\alpha_4\beta_3\delta$ $GABA_ARs$. Left, Representative traces of the currents evoked by 10 mM, 300 μM, and 300 μM GABA followed by application of 10 μM picrotoxin in $\alpha_4\beta_1\delta$-, $\alpha_4\beta_2\delta$-, and $\alpha_4\beta_3\delta$-expressing oocytes, respectively. Right, Averaged levels of constitutive activity in oocytes expressing human $\alpha_4\beta_1\delta$, $\alpha_4\beta_2\delta$, and $\alpha_4\beta_3\delta$ $GABA_ARs$. Constitutive activity is given as the percentage difference between the basal line and the outward current caused by application of 10 μM picrotoxin. Data are mean ± SEM ($n = 6$, $n = 6$, and $n = 4$ for $\alpha_4\beta_1\delta$, $\alpha_4\beta_2\delta$, and $\alpha_4\beta_3\delta$, respectively).

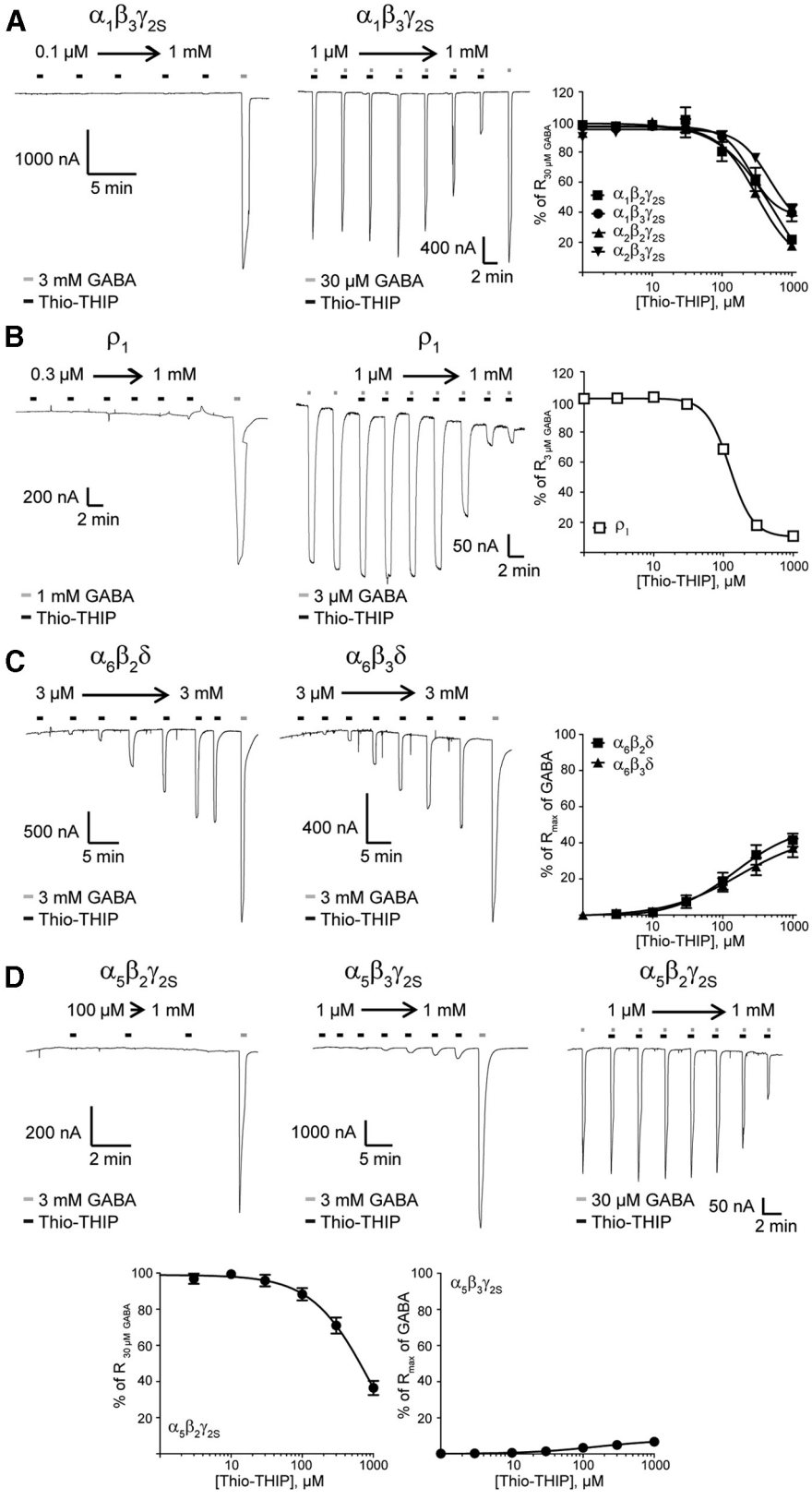

Figure 3. Functional properties of Thio-THIP at various human $GABA_ARs$ expressed in *Xenopus* oocytes. ***A***, The $\alpha_{1,2}\beta_{2,3}\gamma_{2S}$ $GABA_ARs$. Left, Representative traces of the currents evoked by various concentrations of Thio-THIP at the $\alpha_1\beta_3\gamma_{2S}$ $GABA_AR$. Middle, Representative traces of the currents elicited by 30 μM GABA at the $\alpha_1\beta_3\gamma_{2S}$ $GABA_AR$ in the presence of various concentrations of Thio-THIP. Right, Averaged concentration–inhibition curves for Thio-THIP at the $\alpha_1\beta_2\gamma_{2S}$, $\alpha_1\beta_3\gamma_{2S}$, $\alpha_2\beta_2\gamma_{2S}$, and $\alpha_2\beta_3\gamma_{2S}$ $GABA_ARs$ using 30 μM GABA as agonist. Data are mean ± SEM ($\alpha_1\beta_2\gamma_{2S}$: $n = 3$; $\alpha_1\beta_3\gamma_{2S}$: $n = 8$; $\alpha_2\beta_2\gamma_{2S}$: $n = 4$; $\alpha_2\beta_3\gamma_{2S}$: $n = 3$). ***B***, The ρ_1 $GABA_AR$. Left, Representative traces of the currents evoked by various concentrations of Thio-THIP at the ρ_1 $GABA_AR$. Middle, Representative traces of the currents elicited by 3 μM GABA at the ρ_1 $GABA_AR$ in the presence of various concentrations of Thio-THIP. Right, Averaged concentration–inhibition curve for Thio-THIP at the ρ_1 $GABA_AR$ using 3 μM GABA as agonist. Data are mean ± SEM ($n = 4$). ***C***, The $\alpha_6\beta_{2,3}\delta$ $GABA_ARs$. Left, Representative traces of the currents evoked by various concentrations of Thio-THIP at $\alpha_6\beta_2\delta$ and $\alpha_6\beta_3\delta$ $GABA_ARs$. Right, Averaged concentration–response curves for Thio-THIP at the $\alpha_6\beta_2\delta$ and $\alpha_6\beta_3\delta$ $GABA_ARs$. Data are mean ± SEM ($\alpha_6\beta_2\delta$: $n = 3$; $\alpha_6\beta_3\delta$: $n = 4$). ***D***, The $\alpha_5\beta_{2,3}\gamma_{2S}$ $GABA_ARs$. Top, Representative traces of the currents evoked by various concentrations of Thio-THIP at $\alpha_5\beta_2\gamma_{2S}$ and $\alpha_5\beta_3\gamma_{2S}$ $GABA_ARs$ (left and middle), and representative traces of the currents elicited by 30 μM GABA at the $\alpha_5\beta_2\gamma_{2S}$ $GABA_AR$ in the presence of various concentrations of Thio-THIP (right). Bottom, Averaged concentration–inhibition curve for Thio-THIP at the $\alpha_5\beta_2\gamma_{2S}$ $GABA_AR$ using 30 μM GABA as agonist (left) and averaged concentration–response curve for Thio-THIP at the $\alpha_5\beta_3\gamma_{2S}$ $GABA_AR$ (right). Data are mean ± SEM ($\alpha_5\beta_2\gamma_{2S}$: $n = 6$; $\alpha_5\beta_3\gamma_{2S}$: $n = 6$).

sponses than GABA at the receptors (Table 1). THIP displayed monophasic concentration–response relationships at $\alpha_4\beta_2\delta$ and $\alpha_4\beta_3\delta$, whereas the agonist exhibited biphasic or triphasic concentration–response profiles at $\alpha_4\beta_1\delta$-expressing oocytes, neither of which reached saturation at THIP concentrations up to 10 mM (Fig. 2*B–D*). A final substantial difference was the degrees of spontaneous activity exhibited by the three $\alpha_4\beta\delta$ subtypes. Whereas pronounced levels of constitutive activity were observed in oocytes expressing $\alpha_4\beta_1\delta$ and $\alpha_4\beta_3\delta$ receptors, $\alpha_4\beta_2\delta$-expressing oocytes did not display significant levels of spontaneous activity (Fig. 2*E*).

A number of previous studies have reported a wide range of functional potencies and monophasic as well as biphasic concentration–response profiles for both GABA and THIP at $\alpha_4\beta_3\delta$ $GABA_ARs$ expressed in oocytes (Borghese et al., 2006; Stórustovu and Ebert, 2006; Meera et al., 2009, 2011; Hoestgaard-Jensen et al., 2010; Karim et al., 2012, 2013; Hoestgaard-Jensen et al., 2013; Patel et al., 2014), which contrasts the monophasic concentration–response relationships and high-nanomolar and mid-micromolar EC_{50} values consistently displayed by GABA and THIP, respectively, at $\alpha_4\beta_3\delta$ receptors expressed in HEK293 cells (Brown et al., 2002; Mortensen et al., 2004; Meera et al., 2009; Mortensen et al., 2010). The formation of both "high-affinity" and "low-affinity" $\alpha_4\beta_3\delta$ receptors in oocytes has been proposed to arise from the possible formation of multiple $\alpha_4\beta_3\delta$ stoichiometries or subunit arrangements or from the coexpression of $\alpha_4\beta_3\delta$ and "pure" $\alpha_4\beta_3$ complexes (Meera et al., 2009; Karim et al., 2012, 2013). To address whether the considerable range in maximal current amplitudes (200–3500 nA) evoked by

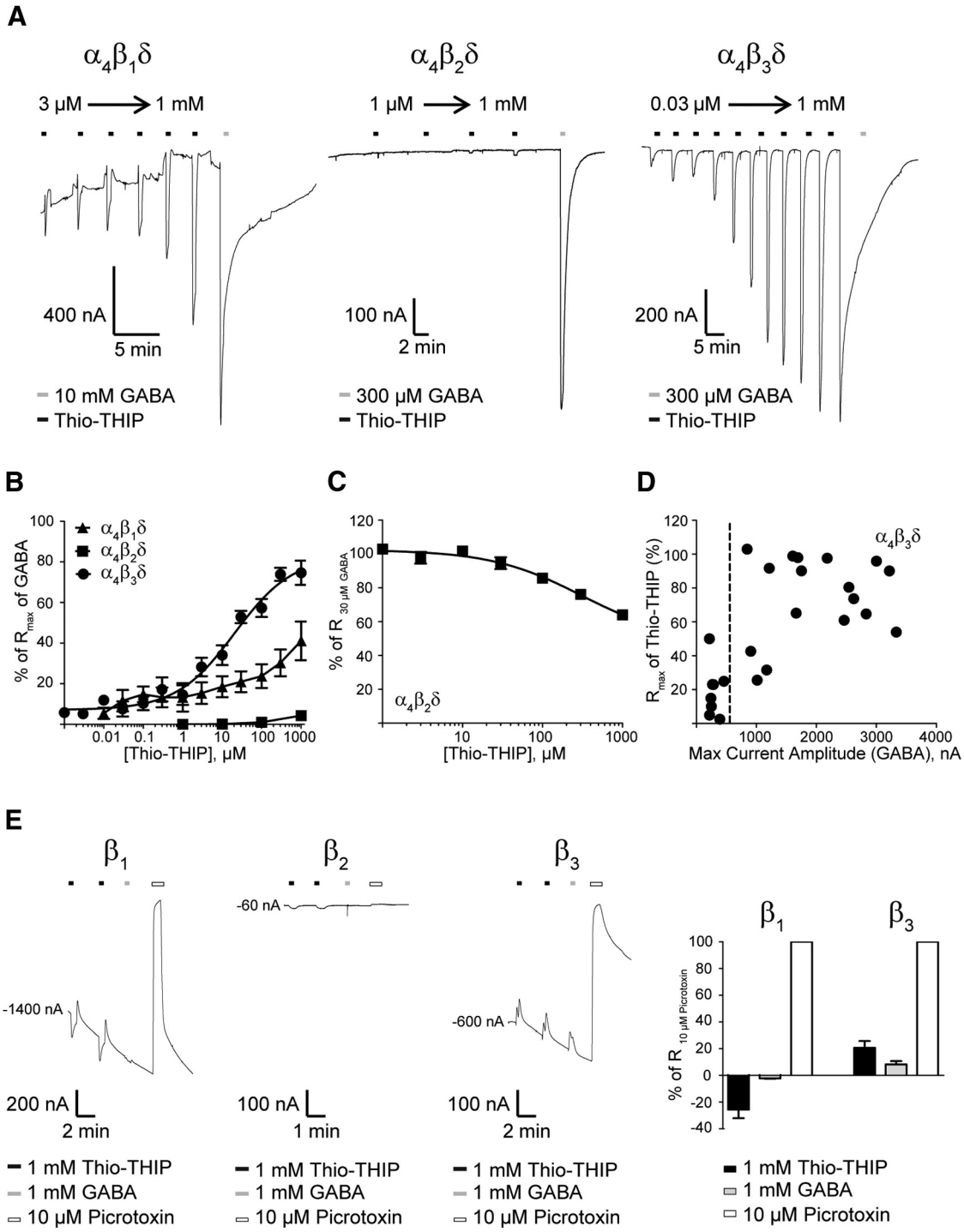

Figure 4. Functional properties of Thio-THIP at human $\alpha_4\beta\delta$ $GABA_ARs$ expressed in *Xenopus* oocytes. ***A***, Representative traces of the currents evoked by various concentrations of Thio-THIP at human $\alpha_4\beta_1\delta$, $\alpha_4\beta_2\delta$, and $\alpha_4\beta_3\delta$ $GABA_ARs$. ***B***, Averaged concentration–response curves for Thio-THIP at the $\alpha_4\beta_1\delta$, $\alpha_4\beta_2\delta$, and $\alpha_4\beta_3\delta$ $GABA_ARs$. Data are mean ± SEM ($\alpha_4\beta_1\delta$: $n = 8$; $\alpha_4\beta_2\delta$: $n = 7$; $\alpha_4\beta_3\delta$: $n = 13$). ***C***, Averaged concentration–inhibition curve for Thio-THIP at the $\alpha_4\beta_2\delta$ $GABA_AR$ using 30 μM GABA as agonist. Data are mean ± SEM ($n = 5$). ***D***, Correlation between the maximum current amplitude evoked by GABA and the R_{max} values of Thio-THIP (in percentage of R_{max} of GABA) at $\alpha_4\beta_3\delta$-expressing oocytes ($n = 25$). The vertical hatched line indicates the differentiation between the recordings where GABA exhibited maximal current amplitudes higher than and lower than 500 nA. ***E***, Representative traces of the currents evoked by 1 mM Thio-THIP, 1 mM GABA, and 10 μM picrotoxin at the human β_1, β_2, and β_3 $GABA_ARs$ (left), and averaged currents evoked by 1 mM Thio-THIP, 1 mM GABA, and 10 μM picrotoxin at the human β_1 and β_3 $GABA_ARs$ (right). Data are mean ± SEM in percentage of the response evoked by 10 μM picrotoxin in the oocyte (β_1: $n = 4$; β_2: $n = 6$; β_3: $n = 5$).

GABA in $\alpha_4\beta_3\delta$-expressing oocytes in this study could arise from mixed $\alpha_4\beta_3\delta/\alpha_4\beta_3$ receptor populations being expressed in some of the oocytes, we investigated the zinc sensitivities of the cell surface-expressed receptors in oocytes at which GABA exhibited maximal current amplitudes lower or higher than 500 nA (Stórustovu and Ebert, 2006). Zn^{2+} (1 μM) was found to exert comparable small degrees of inhibition of the currents evoked by 300 μM GABA in these two oocyte populations, reducing the

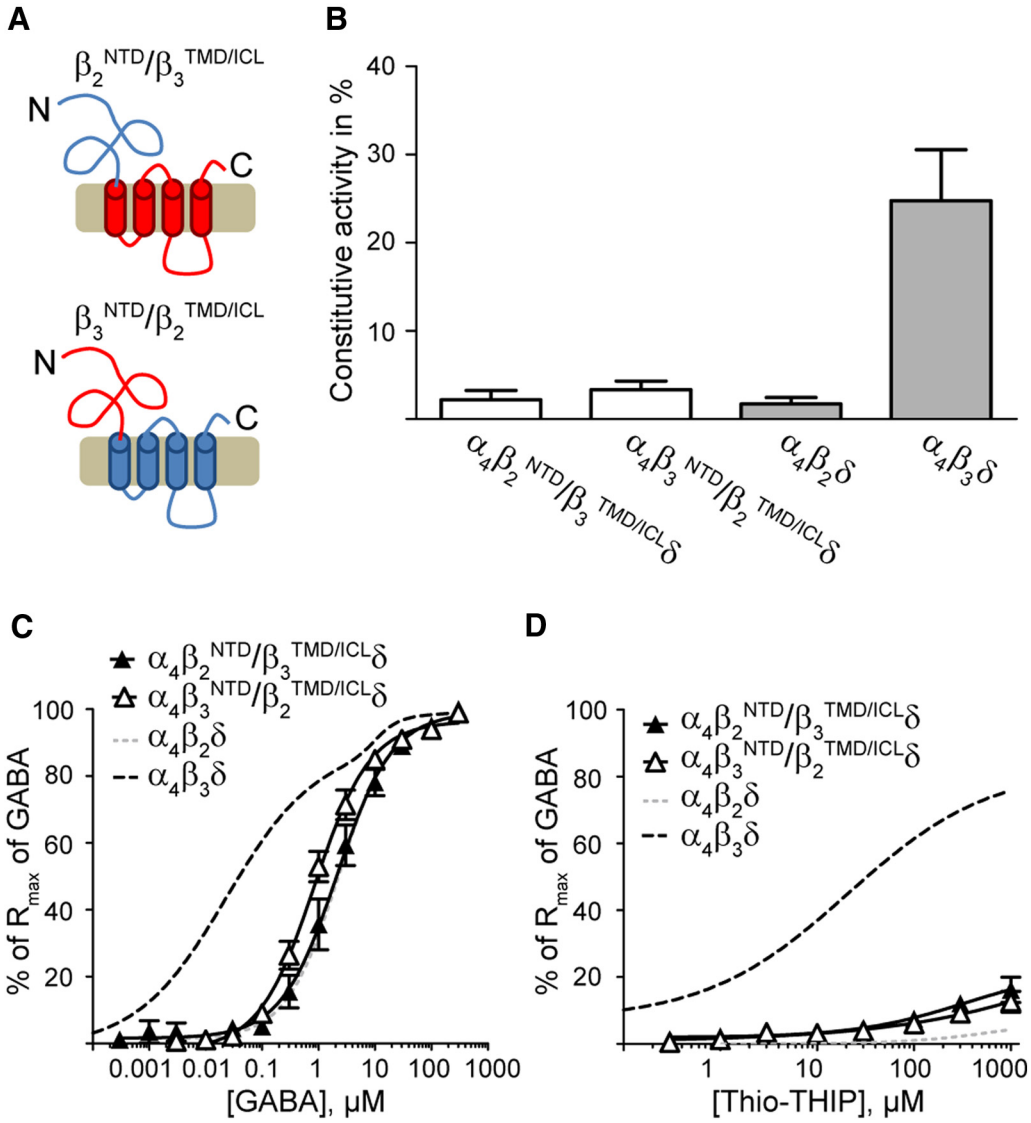

Figure 5. Functional properties of Thio-THIP at human $\alpha_4\beta\delta$ $GABA_ARs$ comprising the chimeric $\beta_2^{NTD}/\beta_3^{TMD/ICL}$ and $\beta_3^{NTD}/\beta_2^{TMD/ICL}$ subunits in *Xenopus* oocytes. ***A***, Schematic representation of the topologies of the $\beta_{2/3}$ and $\beta_{3/2}$ chimeras. The β_2 and β_3 segments in the two chimeras are given in blue and red, respectively. ***B***, Averaged levels of constitutive activity in oocytes expressing $\alpha_4\beta_2^{NTD}/\beta_3^{TMD/ICL}\delta$ and $\alpha_4\beta_3^{NTD}/\beta_2^{TMD/ICL}\delta$ $GABA_ARs$. Constitutive activity is given as the percentage difference between the basal line and the outward current caused by application of 10 μM picrotoxin. Data are mean ± SEM ($\alpha_4\beta_2^{NTD}/\beta_3^{TMD/ICL}\delta$: $n = 3$; $\alpha_4\beta_3^{NTD}/\beta_2^{TMD/ICL}\delta$: $n = 4$). The constitutive activity in oocytes expressing WT $\alpha_4\beta_2\delta$ and $\alpha_4\beta_3\delta$ $GABA_ARs$ (depicted in Fig. 2*E*) is given in gray for comparison. ***C***, Averaged concentration–response curves for GABA at $\alpha_4\beta_2^{NTD}/\beta_3^{TMD/ICL}\delta$ and $\alpha_4\beta_3^{NTD}/\beta_2^{TMD/ICL}\delta$ $GABA_ARs$. Data are mean ± SEM ($\alpha_4\beta_2^{NTD}/\beta_3^{TMD/ICL}\delta$: $n = 6$; $\alpha_4\beta_3^{NTD}/\beta_2^{TMD/ICL}\delta$: $n = 5$). The averaged concentration–response curves for GABA at WT $\alpha_4\beta_2\delta$ and WT $\alpha_4\beta_3\delta$ (depicted in Fig. 2*B*) are given in gray-tone hatched curves for comparison. ***D***, Averaged concentration–response curves for Thio-THIP at the $\alpha_4\beta_2^{NTD}/\beta_3^{TMD/ICL}\delta$ and $\alpha_4\beta_3^{NTD}/\beta_2^{TMD/ICL}\delta$ $GABA_ARs$. Data are mean ± SEM ($\alpha_4\beta_2^{NTD}/\beta_3^{TMD/ICL}\delta$: $n = 7$; $\alpha_4\beta_3^{NTD}/\beta_2^{TMD/ICL}\delta$: $n = 8$). The averaged concentration–response curves for Thio-THIP at WT $\alpha_4\beta_2\delta$ and WT $\alpha_4\beta_3\delta$ (depicted in Fig. 4*B*) are given in gray-tone hatched curves for comparison.

response in ">500 nA" and "<500 nA" $\alpha_4\beta_3\delta$-oocytes to 91 ± 5% ($n = 7$) and 90 ± 1% ($n = 4$) of that recorded in the absence of zinc, respectively. This strongly suggests that few (if any) $\alpha_4\beta_3$ complexes are assembled in these $\alpha_4\beta_3\delta$-oocytes and that the contribution of these receptors to the observed currents thus is negligible. Furthermore, as will be outlined below, the functional properties of the $\alpha_4\beta_3\delta$ receptors did not seem to arise from the formation of homomeric β_3 receptors in the oocytes. On the other hand, we cannot exclude the possibility that different $\alpha_4\beta_3\delta$ receptor complexes (in terms of positional subunit arrangement or subunit stoichiometry) are assembled in the oocytes. This consideration also applies for the receptors formed in $\alpha_4\beta_1\delta$-expressing oocytes, and analogously to $\alpha_4\beta_3\delta$ both "high-affinity" and "low-affinity" $\alpha_4\beta_1\delta$ assemblies have been observed in previous studies (Lovick et al., 2005; Karim et al., 2012; Anstee et al., 2013).

Functional properties of Thio-THIP at human $GABA_ARs$ expressed in *Xenopus* oocytes

In contrast to the concentration-dependent increases in current amplitudes observed for GABA in oocytes expressing $\alpha_1\beta_2\gamma_{2S}$, $\alpha_1\beta_3\gamma_{2S}$, $\alpha_2\beta_2\gamma_{2S}$, and $\alpha_2\beta_3\gamma_{2S}$ $GABA_ARs$, Thio-THIP did not elicit significant agonist responses at any of these four receptors at concentrations up to 1 mM (exemplified for $\alpha_1\beta_3\gamma_{2S}$ in Fig. 3*A*). Instead, the compound was found to be a weak antagonist exhibiting high-micromolar IC_{50} values at the receptors (Fig. 3*A*; Table 1). The inhibitory potencies displayed by Thio-THIP at these four receptors concur with the weak antagonism observed for the

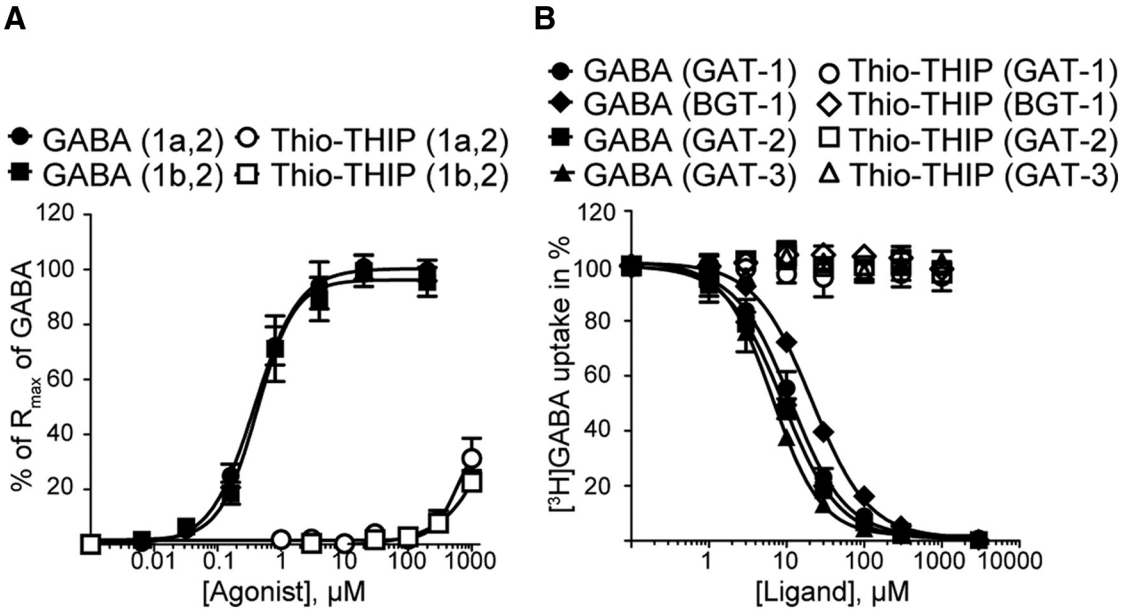

Figure 6. Functional properties of Thio-THIP at $GABA_B$ receptors and GABA transporters. ***A***, Concentration–response relationships for GABA and Thio-THIP at rat $GABA_{B(1a,2)}$ and $GABA_{B(1b,2)}$ receptors coexpressed with the chimeric G-protein $G\alpha_{qi5}$ in tsA201 cells in the Ca^{2+}/Fluo-4 assay. Data are mean ± SEM ($n = 3$ for all). ***B***, Concentration–inhibition relationships for GABA and Thio-THIP at human GAT-1, BGT-1, GAT-2, and GAT-3 transporters stably expressed in Flp-In-CHO cells in the [^{3}H]GABA uptake assay. Data are mean ± SEM ($n = 4$ for all).

compound at the $\alpha_3\beta_2\gamma_2$ $GABA_AR$ in a previous study (Brehm et al., 1997). Whereas applications of Thio-THIP in concentrations up to 300 μM did not evoke significant responses in oocytes expressing the homomeric ρ_1 $GABA_AR$, 1 mM Thio-THIP gave rise to minute but significant currents (Fig. 3*B*; Table 1). When tested as an antagonist at the receptor using GABA (3 μM) as agonist, Thio-THIP exhibited an IC_{50} value of ~150 μM (Fig. 3*B*; Table 1). This *de facto* antagonism is in good agreement with the weak competitive antagonism exhibited by its close structural analog THIP at this receptor (Woodward et al., 1993; Vien et al., 2002).

In contrast to its antagonist activities at the $\alpha_{1,2,3}\beta_{2,3}\gamma_2$ and ρ_1 $GABA_ARs$, Thio-THIP was found to be a partial agonist at the $\alpha_6\beta_2\delta$ and $\alpha_6\beta_3\delta$ subtypes displaying high-micromolar EC_{50} values and maximal responses of ~50% of those of GABA at the two receptors (Fig. 3*C*; Table 1). Interestingly, Thio-THIP displayed pronounced functional selectivity between the β_2- and β_3-containing $\alpha_5\beta\gamma_{2S}$ subtypes. Whereas the compound was a weak antagonist at $\alpha_5\beta_2\gamma_{2S}$, eliciting no significant currents through this receptor at concentrations up to 1 mM, it was an agonist, albeit a low-efficacious one, at the $\alpha_5\beta_3\gamma_{2S}$ receptor (Fig. 3*D*; Table 1). We consider the previously reported antagonist activity of Thio-THIP at $\alpha_5\beta_3\gamma_2$ (Brehm et al., 1997) to be reconcilable with the small intrinsic agonist activity exhibited by the compound at the receptor in this study.

The functional properties displayed by Thio-THIP at the three $\alpha_4\beta\delta$ $GABA_AR$ subtypes were even more diverse than those at the $\alpha_5\beta\gamma_{2S}$ receptors. The compound was a moderately potent partial agonist at the $\alpha_4\beta_3\delta$ receptor exhibiting an EC_{50} of 13 μM and an R_{max} value of 58 ± 7% of that of GABA (Fig. 4*A*,*B*; Table 1). Thio-THIP was also a partial agonist at the $\alpha_4\beta_1\delta$ $GABA_AR$, albeit not as efficacious at this receptor as at $\alpha_4\beta_3\delta$. The compound displayed a biphasic concentration–response relationship at the receptor with a second phase that was not always saturated at concentrations up to 1 mM (Fig. 4*A*,*B*; Table 1). In contrast, application of Thio-THIP at concentrations up to 100 μM did not evoke significant currents in $\alpha_4\beta_2\delta$-expressing oocytes, and 1 mM Thio-THIP only gave rise to a minute response (4 ± 1% of R_{max} of GABA). In concordance with this negligible agonist activity, Thio-THIP was a *de facto* antagonist exerting small but significant inhibition of the GABA EC_{80}-evoked signaling in $\alpha_4\beta_2\delta$-oocytes when applied at concentrations of ≥100 μM (Fig. 4*C*; Table 1). Interestingly, Thio-THIP was a weak low-efficacious partial agonist at the binary $\alpha_4\beta_3$ $GABA_AR$ (Table 1). This suggests that the presence of δ in the $\alpha_4\beta_3\delta$ complex is of key importance for the high-efficacy agonist properties of Thio-THIP at the receptor, a finding that contrasts the comparable agonist efficacies displayed by THIP at $\alpha_4\beta_3$ and $\alpha_4\beta_3\delta$ $GABA_ARs$ in a previous study (Stórustovu and Ebert, 2006).

It should be mentioned that the agonist efficacies displayed by Thio-THIP at the 25 $\alpha_4\beta_3\delta$-expressing oocytes recorded from in this study varied considerably, and a pronounced correlation existed between the R_{max} values determined for Thio-THIP and the maximum current amplitudes evoked by GABA at the respective oocytes (Fig. 4*D*). Because the zinc sensitivities exhibited by receptors in oocytes characterized by both high and low maximal current amplitudes strongly suggest that the receptors in both populations comprise the δ subunit, the differential Thio-THIP efficacies could be speculated to arise from the assembly of different $\alpha_4\beta_3\delta$ receptor populations in terms of subunit stoichiometry or arrangement in the individual oocytes. Nevertheless, it is important to stress that the averaged R_{max} value for Thio-THIP based on all recordings on $\alpha_4\beta_3\delta$ oocytes (58 ± 7%, $n = 25$) supports the claim of Thio-THIP exhibiting substantial agonist efficacy at the $\alpha_4\beta_3\delta$ $GABA_AR$ (Table 1).

In a final set of experiments, Thio-THIP was characterized functionally at human homomeric β_1, β_2, and β_3 $GABA_ARs$, in part to delineate its pharmacology at these receptors and in part to assess the putative contributions of these homomeric β assemblies in $\alpha_4\beta_1\delta$, $\alpha_4\beta_2\delta$, and $\alpha_4\beta_3\delta$ oocytes to the observed functional properties of Thio-THIP. Previous studies of homomeric expression of β_2 in mammalian cell lines and in *Xenopus* oocytes have found the subunit to be retained within the endoplasmic reticulum and thus not being expressed at the cell surface (Connolly et al., 1996; Taylor et al., 1999). In agreement with this,

neither 10 μM picrotoxin, nor 1 mM GABA, nor 1 mM Thio-THIP evoked significant responses in β_2-expressing oocytes (Fig. 4*E*). Also in concordance with previous studies (Sanna et al., 1995; Connolly et al., 1996; Krishek et al., 1996; Simeone et al., 2011), the β_1 and β_3 receptors exhibited high levels of spontaneous activity, as evidenced by the pronounced outward currents produced by application of 10 μM picrotoxin at oocytes expressing these receptors. In contrast, applications of 1 mM GABA did not change the recorded baseline in β_1-expressing oocytes and produced a small outward current in β_3 oocytes (Fig. 4*E*). Interestingly, the effects of 1 mM Thio-THIP on the baselines recorded from β_1 and β_3 oocytes differed, as the compound evoked a small inward current through β_1 and a small outward current through β_3. In conclusion, the putative formation of β_2 homomers clearly does not contribute to the functional properties exhibited by the receptors in $\alpha_4\beta_2\delta$-oocytes. As for β_1 and β_3, the homomeric receptors displayed much more pronounced degrees of constitutive activity than $\alpha_4\beta_1\delta$ and $\alpha_4\beta_3\delta$. More importantly, however, the functional properties exhibited by GABA and Thio-THIP at β_1 and β_3 were strikingly different from those at their respective $\alpha_4\beta\delta$ counterparts. This suggests that, even if homomeric β complexes are assembled in $\alpha_4\beta_1\delta$-and $\alpha_4\beta_3\delta$-oocytes, their contributions to the observed functional properties of these receptors are negligible.

Investigation of the molecular origin of the β isoform-selectivity of Thio-THIP at $\alpha_4\beta\delta$ $GABA_A$Rs

To elucidate the molecular basis for the functional selectivity exhibited by Thio-THIP at the $\alpha_4\beta\delta$ $GABA_A$Rs, the compound was characterized functionally at $\alpha_4\beta\delta$ receptors assembled from the chimeric $\beta_2^{NTD}/\beta_3^{TMD/ICL}$ and $\beta_3^{NTD}/\beta_2^{TMD/ICL}$ subunits. Analogously to the classical chimera between the α7 nicotinic acetylcholine and 5-HT3A receptor subunits (Eiselé et al., 1993), these chimeras consist of the N-terminal domain (NTD) of one β subunit and the transmembrane domain and intracellular loops (TMD/ICL) of the other (Fig. 5*A*). Thus, receptor complexes formed from α_4, $\beta_2^{NTD}/\beta_3^{TMD/ICL}$, and δ subunits will comprise a "pure" $\alpha_4\beta_2\delta$ extracellular domain and "pure" $\alpha_4\beta_3\delta$ ion channel and intracellular domains, and vice versa for $\alpha_4\beta_3^{NTD}/\beta_2^{TMD/ICL}\delta$ receptors.

The basic functional characteristics of the $\alpha_4\beta_2^{NTD}/\beta_3^{TMD/ICL}\delta$ and $\alpha_4\beta_3^{NTD}/\beta_2^{TMD/ICL}\delta$ receptors assembled in oocytes were found to be very similar to those of the WT $\alpha_4\beta_2\delta$ $GABA_A$R (Fig. 5*B*,*C*). Neither of the chimera-containing receptors exhibited significant levels of constitutive activity, and GABA displayed monophasic concentration–response curves at both receptors with EC_{50} values not substantially different from its EC_{50} at WT $\alpha_4\beta_2\delta$ or its $EC_{50,2}$ at WT $\alpha_4\beta_3\delta$ (Fig. 5*B*,*C*; Table 1). Thio-THIP was a distinct agonist at both $\alpha_4\beta_2^{NTD}/\beta_3^{TMD/ICL}\delta$ and $\alpha_4\beta_3^{NTD}/\beta_2^{TMD/ICL}\delta$ displaying efficacies intermediate of those at the two WT receptors, albeit considerably more similar to that at WT $\alpha_4\beta_2\delta$ than at WT $\alpha_4\beta_3\delta$ (Fig. 5*C*; Table 1).

All in all, the agonist properties exhibited by Thio-THIP at the $\alpha_4\beta_2^{NTD}/\beta_3^{TMD/ICL}\delta$ and $\alpha_4\beta_3^{NTD}/\beta_2^{TMD/ICL}\delta$ receptors do not to shed much light on the putative molecular determinants for its $\alpha_4\beta\delta$ subtype selectivity. On one hand, the intermediate agonist efficacies displayed by Thio-THIP at these receptors compared with WT $\alpha_4\beta_2\delta$ and $\alpha_4\beta_3\delta$ could indicate that the functionality of Thio-THIP at the $\alpha_4\beta\delta$ receptor does not arise exclusively from molecular elements in the NTD or the TMD/ICL but from the entire β subunit comprised in the $\alpha_4\beta\delta$ complex. On the other hand, the subunit stoichiometries and/or arrangements of the $\alpha_4\beta_2^{NTD}/\beta_3^{TMD/ICL}\delta$ and $\alpha_4\beta_3^{NTD}/\beta_2^{TMD/ICL}\delta$ receptors cannot be assumed to be identical to those of WT $\alpha_4\beta_2\delta$ and $\alpha_4\beta_3\delta$, just as the subunit stochiometries and arrangements of the two WT receptors may differ. Thus, the fact that both chimera-containing receptors exhibit basic functionalities (low degrees of constitutive activity and monophasic GABA concentration–response curves) and Thio-THIP efficacies comparable with those at WT $\alpha_4\beta_2\delta$ could also be a reflection of these three receptors sharing the same $\alpha_4\beta\delta$ subunit stoichiometry and/or arrangement, and that this differs from that of WT $\alpha_4\beta_3\delta$.

Functional properties of Thio-THIP at other GABAergic targets

The applicability of any ligand as a pharmacological tool in *ex vivo* or *in vivo* studies of $GABA_A$Rs is dependent on its putative off-target effects, and obviously the chance of a compound possessing activity at other GABAergic proteins is particularly prominent when it comes to a GABA analog such as Thio-THIP. To address this issue, we investigated the functional properties of Thio-THIP at the two other classes of membrane-bound GABAergic targets: the $GABA_B$ receptors and the GABA transporters.

The effects of Thio-THIP on $GABA_B$ receptor signaling were studied in a Ca^{2+}/Fluo-4 assay using tsA201 cells coexpressing either the $GABA_{B(1a,2)}$ or the $GABA_{B(1b,2)}$ receptor with $G\alpha_{qi5}$, a chimeric G-protein directing the signaling of the $G\alpha_{i/o}$-protein-coupled $GABA_B$ receptors into the $G\alpha_q$-pathway and intracellular Ca^{2+} mobilization (Conklin et al., 1993). GABA increased fluorescence intensity in this assay in a concentration-dependent manner displaying pEC_{50} (± SEM) values of 6.42 ± 0.08 and 6.38 ± 0.07 at $GABA_{B(1a,2)}$ and $GABA_{B(1b,2)}$, respectively ($n = 3$ for both; Fig. 6*A*). These potencies were comparable with or slightly higher than those previously determined for GABA at $GABA_B$ receptors coexpressed with chimeric G-proteins in inositol phosphate accumulation assays (Bräuner-Osborne and Krogsgaard-Larsen, 1999; Duthey et al., 2002). Thio-THIP was found to be a weak $GABA_B$ receptor agonist evoking small but significant responses through both of the receptors at concentrations of ≥300 μM (Fig. 6*A*).

The putative activity of Thio-THIP as a substrate or an inhibitor at the four human GABA transporters was investigated in a conventional [^{3}H]GABA uptake assay. The inhibitory potencies displayed by GABA at CHO cell lines stably expressing GAT-1 (pIC_{50} ± SEM: 4.94 ± 0.07, $n = 4$), BGT-1 (pIC_{50} ± SEM: 4.67 ± 0.11, $n = 4$), GAT-2 (pIC_{50} ± SEM: 5.04 ± 0.06, $n = 4$), and GAT-3 (pIC_{50} ± SEM: 5.18 ± 0.06, $n = 4$) in this assay were in good agreement with previous findings (Fig. 6*B*) (Kvist et al., 2009). Thio-THIP did not exert significant inhibition of the [^{3}H]GABA uptake through any of the four transporters at concentrations up to 1 mM (Fig. 6*B*).

Functional characterization of Thio-THIP at native $GABA_A$Rs in rat brain slices

We found the functional profile exhibited by Thio-THIP at the recombinant human $GABA_A$Rs highly interesting, in particular its ability to discriminate between the three $\alpha_4\beta\delta$ receptor subtypes. To investigate to which extent this *in vitro* profile of the compound translated into its functionality at native $GABA_A$Rs and to probe its potential as a pharmacological tool, we assessed the effects of Thio-THIP on synaptic and extrasynaptic $GABA_A$Rs in different rat brain regions (Fig. 7*A*,*B*). A concentration of 100 μM Thio-THIP was used in these recordings because the *in vitro* profile of the compound suggests that this concentration will give rise to robust activation of $\alpha_4\beta_1\delta$ and $\alpha_4\beta_3\delta$ receptors and negligible inhibition of the $\alpha_4\beta_2\delta$ $GABA_A$R, and that, besides modest activa-

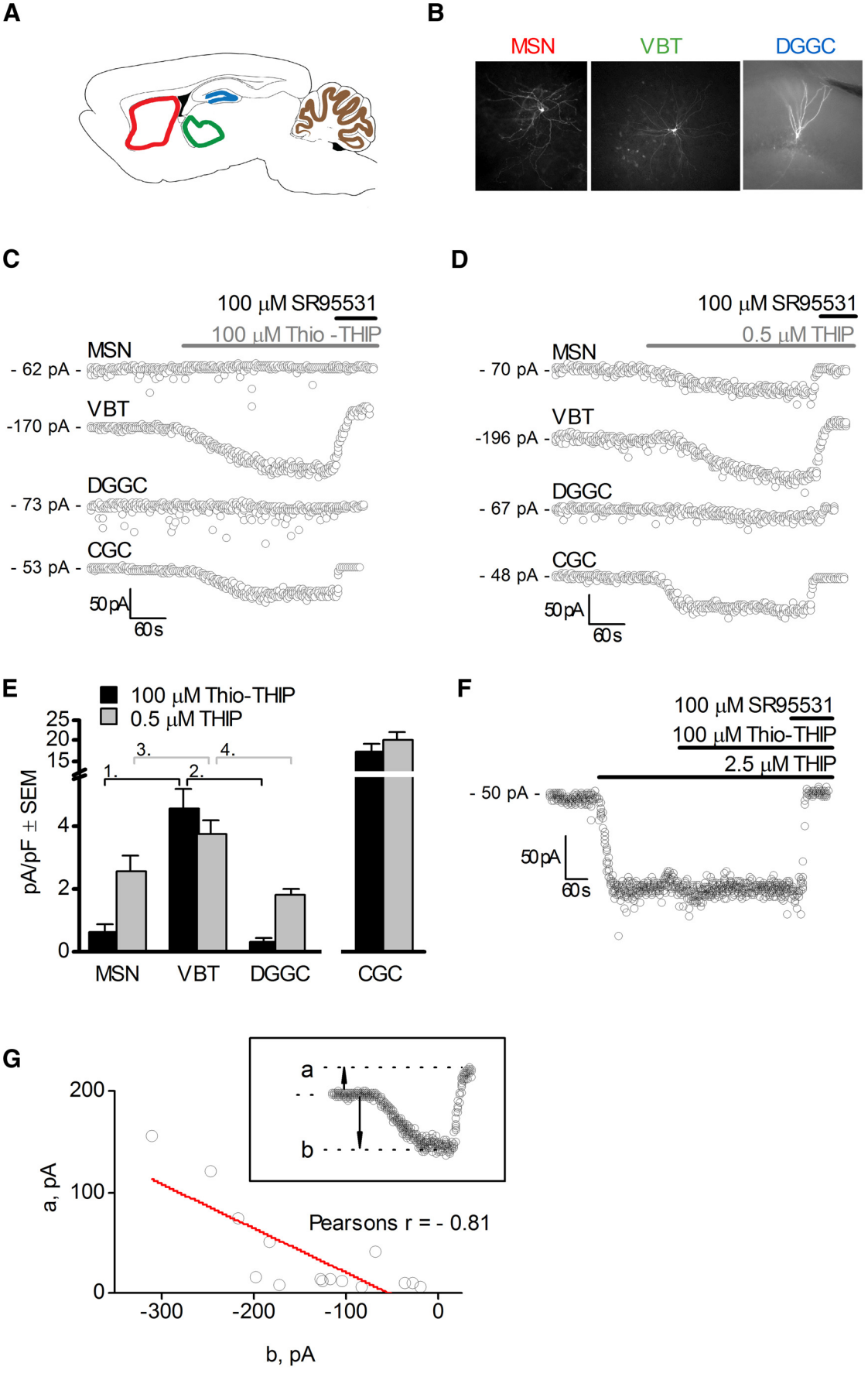
A
B
MSN
VBT
DGGC
C
100 μM SR95531
100 μM Thio -THIP
MSN
- 62 pA -
VBT
-170 pA -
DGGC
- 73 pA -
CGC
- 53 pA -
50 pA
60 s
D
100 μM SR95531
0.5 μM THIP
MSN
- 70 pA -
VBT
-196 pA -
DGGC
- 67 pA -
CGC
- 48 pA -
50 pA
60 s
E
100 μM Thio-THIP
0.5 μM THIP
pA/pF ± SEM
25
20
15
4
2
0
1.
2.
3.
4.
MSN
VBT
DGGC
CGC
F
100 μM SR95531
100 μM Thio-THIP
2.5 μM THIP
- 50 pA -
50 pA
60 s
G
a
b
200
100
0
a, pA
-300
-200
-100
0
b, pA
Pearsons r = - 0.81

Table 2. Current densities recorded in four different rat brain regions using THIP or Thio-THIP[a]

		THIP	
	100 μM Thio-THIP	0.5 μM	2.5 μM
CGCs	17.5 ± 1.8 (6)	20.1 ± 2.0 (5)	NT
VBT cells	4.6 ± 0.6 (15)	3.8 ± 0.4 (5)	15.0 ± 2.6 (5)
DGGCs	0.3 ± 0.1 (8)	1.8 ± 0.2 (5)	4.9 ± 0.8 (6)
Striatal MSNs	0.6 ± 0.3 (7)	2.6 ± 0.5 (7)	7.1 ± 0.6 (9)

[a]Data are given as mean ± SEM values in pA/pF (number of recordings forming the basis for the respective values in parentheses). NT, Not tested.

tion of the $\alpha_6\beta_{2,3}\delta$ receptors, it will have negligible effects on other mediators of GABAergic neurotransmission ($\alpha_{1,2,3,5}\beta_{2,3}\gamma_2$ receptors, $GABA_B$ receptors, and GABA transporters).

Effects of Thio-THIP on the $GABA_A$Rs mediating tonic inhibition

In these recordings, the capacitance ranges of the neurons used to normalize the respective effects of the test compounds on holding current were 2–4 pF ($n = 11$) for cerebellar granule cells (CGCs), 8–12 pF ($n = 23$) for striatal medium spiny neurons (MSNs), 9–13 pF ($n = 19$) for dentate gyrus granule cells (DGGCs), and 11–18 pF ($n = 25$) for principal cells of ventrobasal thalamus (VBT). In our recordings from striatal MSNs in the anterior dorsal region of caudate–putamen, we did not differentiate between striatonigral MSNs expressing dopamine D_1 receptors (D_1 + MSNs) and striatopallidal MSNs expressing dopamine D_2 receptors (D_2 + MSNs). For all striatal MSNs and DGGCs, addition of SR95531 to the bath was observed to silence all synaptic currents and restore the holding current of the cell (if changed by the applied drug) to its initial value. In contrast, in 10 of 25 VBT neurons and in 6 of 13 CGCs recorded from, the response to SR95531 was a more positive holding current than the baseline, which most likely reflects the baseline GABA-induced tonus on extrasynaptic receptors in these regions (Fig. 7*C*,*D*). The use of the functionally selective $\alpha_4\beta\delta/\alpha_6\beta\delta$ receptor agonist THIP as a reference ligand in these recordings served partly to verify that currents mediated by extrasynaptic δ-$GABA_A$Rs could indeed be recorded from the patched cells and partly as a reference to which the observed effects of Thio-THIP could be related. In concordance with its extensive use in previous studies of extrasynaptic $\alpha_4\beta\delta$ and $\alpha_6\beta\delta$ receptors, 0.5 and 2.5 μM THIP were found to elicit robust currents in all four rat brain regions (Fig. 7*D*; Table 2).

In contrast to the uniform induction of currents by THIP in the four cell types, 100 μM Thio-THIP had highly differential effects on the currents in the four regions. Thio-THIP evoked robust inward currents in CGCs comparable in size with those elicited by 0.5 μM THIP (Fig. 7*C–E*; Table 2). In contrast, the compound did not induce significant currents in striatal MSNs or in DGGCs (Fig. 7*C–E*; Table 2). To investigate whether Thio-THIP possesses antagonistic effects at the extrasynaptic receptors in striatal MSNs, we used a scheme of application of 2.5 μM THIP until stable current was obtained followed by coapplication of 2.5 μM THIP and 100 μM Thio-THIP. As can be seen from Figure 7*F*, the THIP-induced currents in striatal MSNs were not reduced by the presence of Thio-THIP, as the change in holding current upon the coaddition of 100 μM Thio-THIP was negligible (6.4 ± 5.1 pA, $n = 4$).

In VBT neurons, 100 μM Thio-THIP induced substantial currents characterized by an average current density comparable with those elicited by 0.5 μM THIP (4.6 ± 0.6 pA/pF and 3.8 ± 0.4 pA/pF, respectively) (Fig. 7*C–E*). One-way ANOVA of the current density for the MSN, DGGC, and VBT groups in 100 μM Thio-THIP gave $F = 16.9$ and $p = 9.9E\text{-}6$, and *post hoc* Bonferroni test gave $p = 8E\text{-}5$ (VBT vs DGGC), $p = 4E\text{-}4$ (VBT vs MSN) and $p = 1$ (DGGC vs MSN). Thus, the average current density observed for 100 μM Thio-THIP in VBT neurons was 7.7- and 15.3-fold higher than those recorded from striatal MSNs or DGGCs, respectively. In comparison, analysis of the differences in current densities observed for 0.5 μM THIP in the three cell types gave $F = 6.8$ and $p = 0.01$ (one-way ANOVA) and Bonferroni test gave $p = 0.01$ (VBT vs DGGC) but $p = 0.18$ (VBT vs MSN) and $p = 0.4$ (DGGC vs MSN), indicating a 2.1-fold larger current density in VBT cells than in DGGCs. Interestingly, the current densities evoked by Thio-THIP in the 15 VBT cells recorded from in this study varied greatly and so did the degrees of basal activity observed for the respective neurons (assessed by the inward currents induced by 100 μM SR95531). Interestingly, a pronounced correlation was observed between the sizes of these two parameters from the VBT neuron recordings (Fig. 7*G*).

Effects of Thio-THIP on the $GABA_A$Rs mediating phasic inhibition

To characterize the effects of Thio-THIP on the $GABA_A$Rs mediating phasic currents in VBT neurons, DGGCs and striatal MSNs, we analyzed the mIPSCs in the same neurons used for the analysis described in the previous section. A similar analysis of mIPSCs in CGCs could not be performed because the few spontaneous events (<20 during a 3 min period) that could be resolved during baseline conditions in these cells were lost in the noise caused by the Thio-THIP application (unpublished observations). Furthermore, in 3 of the 15 VBT neurons patched, very low frequencies of mIPSCs (<0.1 Hz) were detected, even though the cells displayed similar levels of extrasynaptic $GABA_A$R-mediated currents and similar responses to SR95531 as the 12 other cells (unpublished observations). Thus, these three cells were excluded from the analysis of the synaptic currents.

The properties of the averaged synaptic current in VBT neurons, DGGCs, and striatal MSNs during baseline conditions and in the presence of 100 μM Thio-THIP are given in Table 3, and representative recordings from the cells are depicted in Figure 8*A*. The shape of the averaged synaptic current in the striatal MSN was not affected by the presence of 100 μM Thio-THIP. In the VBT neuron, the presence of Thio-THIP prolonged the decay time of the current significantly (Fig. 8*A*; Table 3). Although the detection limit in these neurons is based upon the noise level (SD) in the drug period, an increased noise will in particular affect the measurement of the decay time of small mIPSCs. Using a detection limit of 10 × SD, we observed a decay tau of 6.3 ± 0.8 in the

←

Figure 7. Effects of Thio-THIP on the $GABA_A$Rs mediating tonic inhibition in neurons from four rat brain regions: striatal MSNs, principal cells of VBT, DGGCs, and CGCs. ***A***, Schematic representation of the localization of striatum (red), thalamus (green), hippocampus (blue), and cerebellum (brown) in rat brain. ***B***, Micrographs of fluorescence-emitting, biocytin-filled striatal MSNs, VBT cells, and DGGCs. ***C***, Representative traces for the currents induced by 100 μM Thio-THIP in striatal MSNs, VBT cells, DGGCs, and CGCs. ***D***, Representative traces for the currents induced by 0.5 μM THIP in striatal MSNs, VBT cells, DGGCs, and CGCs. ***C***, ***D***, An endogenous current was observed in 10 of 25 VBT neurons and in 6 of 13 CGCs. ***E***, Averaged current densities exhibited 100 μM Thio-THIP and 0.5 μM THIP in striatal MSNs, VBT cells, DGGCs, and CGCs. The current is normalized to the cell capacitance (current density, pA/pF). Groups (bar designated 1–4) were compared for the same compound in different regions: $^{1,2}p < 0.001$; $^{3}p = 0.18$; $^{4}p = 0.01$ (one-way ANOVA, Bonferroni). ***F***, Representative trace exemplifying the lack of effect of 100 μM Thio-THIP on the currents evoked by 2.5 μM THIP in striatal MSNs. ***G***, Correlation between the inward currents induced by 100 μM SR95531 (a) and the currents evoked by 100 μM Thio-THIP (b) in the 15 VBT cells recorded in this study.

Table 3. Properties of mIPSCs in regional principal cells recorded under basal conditions and in the presence of 100 μM Thio-THIP[a]

	VBT cells ($n = 13$)		DGGCs ($n = 8$)		Striatal MSNs ($n = 7$)	
	Baseline	Thio-THIP	Baseline	Thio-THIP	Baseline	Thio-THIP
RT_{20-80} (ms)	0.64 ± 0.06	0.69 ± 0.08	0.44 ± 0.03	0.53 ± 0.05	0.73 ± 0.04	0.81 ± 0.06
Peak (pA)	−20.2 ± 2.6	−18.7 ± 2.8	−35.7 ± 4.2	−25.4 ± 2.9***	−18.1 ± 1.9	−17.4 ± 2.7
Weighted tau (ms)	9.0 ± 0.7	12.4 ± 0.6**	7.3 ± 0.6	8.9 ± 0.6**	13.3 ± 1.6	16.0 ± 1.7
Area (pA × ms)	258 ± 24	323 ± 42*	310 ± 30	271 ± 21*	310 ± 30	344 ± 34

[a]The RT_{20-80}, peak, weighted tau (2 exponentials), and area values are given as mean ± SEM, and the numbers of recordings (*n*) forming the basis for the values for the three cell types are listed.

*$p < 0.05$ (paired *t* test); **$p < 0.01$ (paired *t* test); ***$p < 0.001$ (paired *t* test).

absence and 7.3 ± 0.7 in the presence of Thio-THIP ($p = 0.12$), indicating that increased baseline noise interfere with the measurement of decay time, and this effect is larger for small events.

The most pronounced effect of 100 μM Thio-THIP on synaptic currents observed in this study was the significantly reduced peaks of the mIPSCs recorded in DGGCs in the presence of the compound. In contrast, the compound had only very little effect on the baseline noise (i.e., the detection limit) in these cells (Fig. 8*A*; Table 3). We tested whether it was possible to reverse the effect of Thio-THIP on mIPSC peak in DGGCs after washout, and we found that peak values of 42.9 ± 3.6 pA ($n = 5$) during baseline were reduced to 34.6 ± 3.3 pA during 100 μM Thio-THIP, and again increased to 40.0 ± 3.9 pA, 8 min after washout begin ($p = 0.03$, Thio-THIP vs washout). In a study of mouse DGGCs, Wei et al. (2003) have found δ-containing $GABA_ARs$ (most likely $\alpha_4\beta\delta$ assemblies) to be localized perisynaptically, particularly on the distal part of the apical dendrite (Soltesz et al., 1995). To assess whether the observed effects of Thio-THIP on the recorded mIPSCs could be ascribed to Thio-THIP targeting an analogous receptor population in rat DGGCs, we first tested the sensitivity of mIPSCs to 15 μM Zn^{2+} in phosphate-free buffer. In these recordings ($n = 5$), Thio-THIP had no effect on the RT_{20-80}, peak, or decay characteristics of the averaged mIPSC (Fig. 8*B*). Specifically, the average mIPSC peaks (± SEM) were 41.2 ± 6.8 pA at baseline, 28.9 ± 4.7 pA in the presence of 15 μM Zn^{2+} ($p = 0.01$), and 29.0 ± 4.8 pA in the concomitant presence of 15 μM Zn^{2+} and 100 μM Thio-THIP ($p = 0.9$, Zn^{2+} vs Zn^{2+}/Thio-THIP, paired *t* test). Furthermore, we tested the effects of the addition of the δ-$GABA_AR$-selective PAM DS2 (1 μM) alone and in combination with a submaximal dose of Thio-THIP (25 μM) on these currents. When tested alone, DS2 displayed no effects on peak, decay, or RT_{20-80} ($n = 5$), whereas Thio-THIP (25 μM) prolonged the decay only (6.1 ± 0.2 ms in baseline and 6.9 ± 0.3 ms in 25 μM Thio-THIP, $n = 5$, $p = 0.01$; Fig. 8*C*). Coapplication of 1 μM DS2 and 25 μM Thio-THIP significantly diminished the mIPSC peak (31.4 ± 2.6 in baseline vs 27.4 ± 2.2 in drug combination, $n = 6$, $p = 0.001$) and prolonged the decay (5.7 ± 0.1 ms in baseline vs 6.9 ± 0.4 in drug combination, $n = 6$, $p = 0.01$). Together, this suggests that the reduction in the peak of the average mIPSC observed in the presence of 100 μM Thio-THIP can be ascribed to the compound targeting δ-containing $GABA_ARs$ responsible for a component of the synaptic current in rat DGGCs, possibly perisynaptically localized $\alpha_4\beta\delta$ receptors analogous to those proposed to be expressed in mice DGGC dendrites (Wei et al., 2003). In a final series of experiments, we recorded from dentate hilar subgranular interneurons characterized by large soma (capacitance range 17–26 pF, $n = 3$). Perfusion of 100 μM Thio-THIP to the bath had no effect on the holding current in these cells (2.1 ± 3.6 μA), and peak of the average events was unchanged (28.6 ± 2.4 pA in the absence vs 27.7 ± 2.3 pA in the presence of 100 μM Thio-THIP). Although the absence of an effect from Thio-THIP on one hand could indicate that $\alpha_4\beta_{1,3}\delta$ receptors are not expressed in the cells, activation of the receptors, if indeed expressed, could also be insufficient to trigger significant currents. Thus, we shall refrain from drawing solid conclusions about whether or not these interneurons express $\alpha_4\beta_{1,3}\delta$ receptors based on these data. On the other hand, the lack of effect from Thio-THIP could indicate that the compound does not activate the $\alpha_1\beta\delta$ receptors shown to mediate tonic currents in these interneurons (Glykys et al., 2007), although this will be important to verify at recombinant $\alpha_1\beta\delta$ receptors in heterologous expression systems.

Discussion

The abundant expression and the essential roles of $\alpha_4\beta\delta$ $GABA_ARs$ as mediators of tonic conductance in the CNS make them important contributors to numerous physiological processes and pathophysiological states (Belelli et al., 2009; Brickley and Mody, 2012), and the therapeutic potential of the receptors are substantiated by the *in vivo* effects of THIP and δ-$GABA_AR$ selective PAMs (Ebert et al., 2006; Wafford et al., 2009; Hoestgaard-Jensen et al., 2010). Considering the heterogeneous nature of native $\alpha_4\beta\delta$ receptor populations and the likely differential regulation of the β_1-, β_2-, and β_3-containing subtypes by post-translational processes such as phosphorylation (Kittler and Moss, 2003; Houston et al., 2009), the possibility that the $\alpha_4\beta\delta$ subtypes could mediate distinct physiological functions has attracted surprisingly little attention. In the present study, Thio-THIP has been shown to be a potentially useful tool for investigations of the $\alpha_4\beta\delta$ subtypes and their respective roles in GABAergic neurotransmission.

The distinct subtype selectivity profile of Thio-THIP at recombinant $GABA_ARs$

The different functionalities exhibited by THIP and Thio-THIP at recombinant $GABA_ARs$ are intriguing. Introduction of the sulfur into the heteroaromatic ring of THIP not only transforms its agonism and superagonism at $\alpha_{1,2,3,5}\beta\gamma_2$ and $\alpha_{4,6}\beta\delta$ receptors, respectively, into antagonism and partial agonism, it also converts its nonselective agonist activity at $\alpha_4\beta\delta$ receptors into pronounced $\alpha_4\beta_1\delta/\alpha_4\beta_3\delta$ selectivity. Extensive use of 3-isoxazolol and 3-isothiazolol as carboxylate bioisosteres in the glutamate receptor field has shown that it is virtually impossible to rationalize pharmacological differences arising from this seemingly small structural difference solely by the physicochemical properties of the two ring systems (Matzen et al., 1997; Hermit et al., 2004). Moreover, considering the conserved nature of the orthosteric $GABA_AR$ site, in particular when it comes to the principal $\beta^{(+)}$ binding component (Sieghart, 2006), the β selectivity of Thio-THIP is unlikely to be rooted in substantially different binding interactions with the three $\alpha_4\beta\delta$ subtypes. Instead, it may arise from different energy barriers associated with allosteric transitions between ligand binding and gating in the receptors or from the assembly of different $\alpha_4\beta\delta$ complexes in $\alpha_4\beta_1\delta$-, $\alpha_4\beta_2\delta$-, and

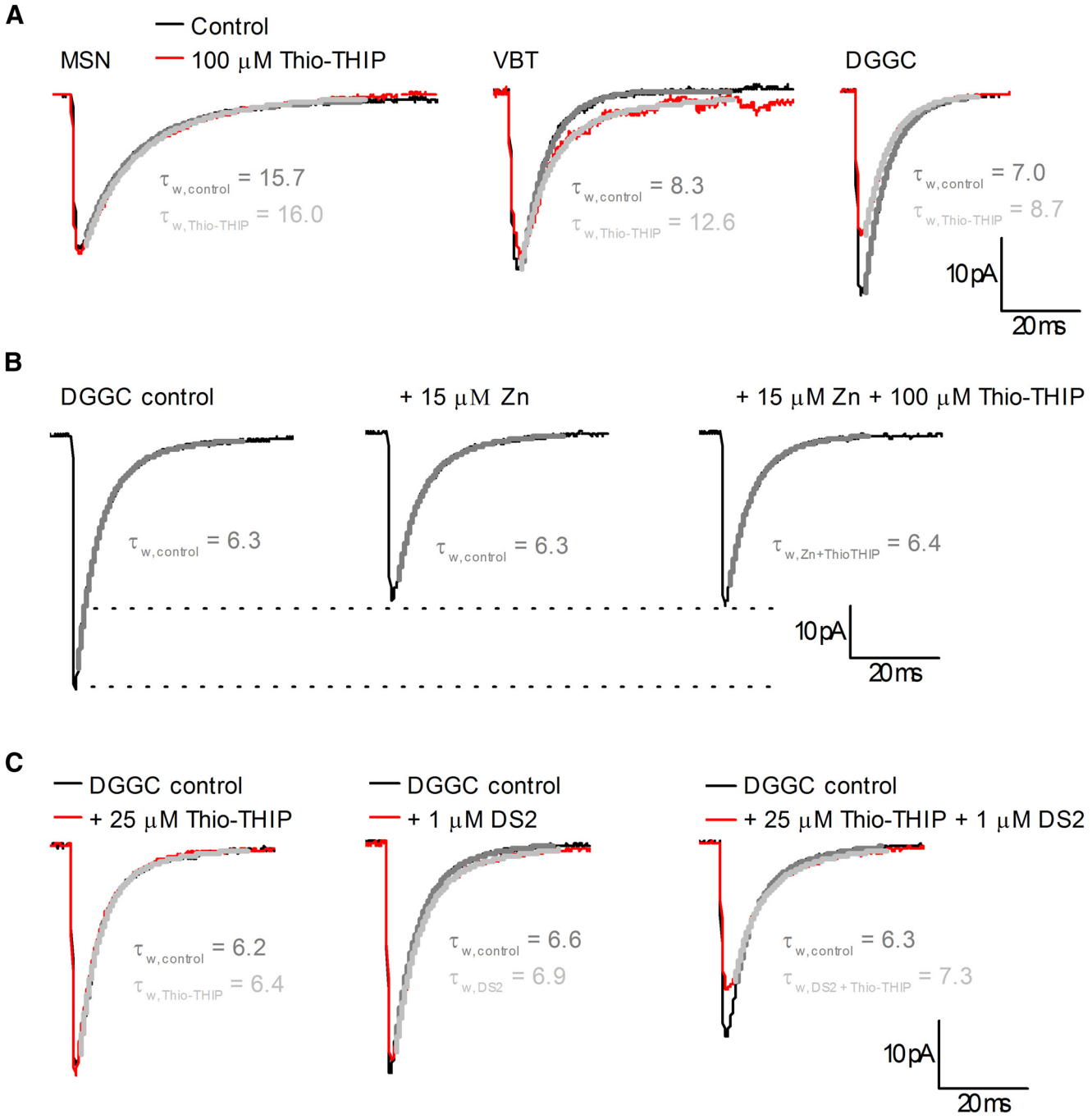

Figure 8. Effects of Thio-THIP on the $GABA_A$Rs mediating phasic inhibition in neurons from three rat brain regions: striatal MSNs, principal cells of VBT, and DGGCs. ***A***, The average noncontaminated waveforms of the mIPSCs recorded from striatal MSNs, VBT cells, and DGGCs in the absence (Control) or in the presence of 100 μM Thio-THIP. ***B***, The average noncontaminated waveforms of the mIPSCs recorded from DGGCs in the absence (Control) or in the presence of 15 μM Zn^{2+} or 15 μM Zn^{2+} and 100 μM Thio-THIP. ***C***, Examples of the average mIPSC waveform of DGGCs exposed to 25 μM Thio-THIP (left), 1 μM DS2 (middle), or the combination (right). The decay time constants are the weighted time constants from fits to a biexponential function.

$\alpha_4\beta_3\delta$-oocytes. $\alpha_4\beta\delta$ $GABA_A$Rs have been reported to assemble as both $\beta\alpha\beta\alpha\delta$ and/or $\beta\alpha\beta\delta\alpha$ pentamers (anticlockwise, viewed from extracellular space) in heterologous expression systems (Barrera et al., 2008; Shu et al., 2012; Eaton et al., 2014; Patel et al., 2014), and concatameric $\alpha_{1,6}\beta_3\delta$ receptors with several different subunit arrangements have also been shown to be functional (Baur et al., 2009; Kaur et al., 2009). Whether all $\alpha_4\beta\delta$ pentamers assembled *in vitro* are expressed in neurons is obviously another matter, and the possible implications of this for Thio-THIP as a pharmacological tool will be addressed below.

The effects of Thio-THIP at native rat $GABA_A$Rs

All in all, the observed effects of Thio-THIP on the currents mediated by synaptic and extrasynaptic $GABA_A$Rs in four rat brain regions are in good agreement with its properties at the recombinant human receptors. Moreover, the observations in the slice recordings not only concurs with previous findings about native $\alpha_4\beta\delta$ $GABA_A$Rs but also sheds further light on the heterogeneity of these receptors.

Extrasynaptic $\alpha_6\beta\delta$ $GABA_A$Rs are the key mediators of tonic inhibition in CGCs (Jones et al., 1997; Brickley et al., 2001), and the robust currents evoked by Thio-THIP in these cells thus con-

cur with its agonist activity at recombinant $\alpha_6\beta_{2,3}\delta$ receptors. $\alpha_4\beta\delta$ $GABA_A$Rs are equally well established as major extrasynaptic receptors in rodent DGGCs (Nusser and Mody, 2002; Stell et al., 2003; Chandra et al., 2006; Zhang et al., 2007). In an elegant study using β_2 knock-out ($\beta_2{}^{-/-}$) and etomidate-insensitive β_2 knock-in ($\beta_{2/N265S}$) mice, $\alpha_4\beta_2\delta$ has been identified as the key mediator of tonic inhibition in these cells, albeit with significant contributions from $\alpha_5\beta_{1/3}\gamma_2$, $\alpha_x\beta_{1/3}$, and/or $\alpha_x\beta_{1/3}\delta$ receptors (Herd et al., 2008). The inability of 100 μM Thio-THIP to activate extrasynaptic receptors in rat DGGCs substantiates the notion of $\alpha_4\beta_2\delta$ being the major extrasynaptic $GABA_AR$ in rodent DGGCs.

The current insight into the compositions of extrasynaptic $GABA_A$Rs in striatal MSNs is largely based on mice studies. α_2, α_4, β_3, and δ are the predominant subunits in adult mouse MSNs, but surprisingly the α_4δ-containing receptors mediating tonic currents here do not appear to comprise β_3 (Janssen et al., 2009; Luo et al., 2013). Single-cell RT-PCR analysis has detected widespread expression of β_1 and β_3 but not of β_2 in adult rat D_1+ MSNs (Flores-Hernandez et al., 2000); and although a concomitant abundant β_1 and β_3 mRNA expression and absence of the two subunits in extrasynaptic $\alpha_4\beta\delta$ assemblies in rat MSNs would be analogous to the observations for β_3 in mouse MSNs, it does call for caution when interpreting our findings. Thus, although the inability of 100 μM Thio-THIP to elicit currents and to block THIP-induced currents in MSNs seems to point to $\alpha_4\beta_2\delta$ as the major extrasynaptic $\alpha_4\beta\delta$ subtype in adult rodent striatal MSNs, it will be important to challenge this conclusion in future studies.

$\alpha_4\beta\delta$ $GABA_A$Rs are the key extrasynaptic/perisynaptic receptors in VBT neurons (Sur et al., 1999; Jia et al., 2005; Chandra et al., 2006; Herd et al., 2009). In concordance with higher expression levels of β_2 than β_1 and β_3 (Laurie et al., 1992; Wisden et al., 1992; Hörtnagl et al., 2013), a study using $\beta_2{}^{-/-}$ and $\beta_{2/N265S}$ mice has identified $\alpha_4\beta_2\delta$ as the predominant extrasynaptic $\alpha_4\beta\delta$ subtype in these neurons (Belelli et al., 2005). The significant currents evoked by 100 μM Thio-THIP in VBT neurons do not necessarily challenge this conclusion, but the observation suggests that $\alpha_4\beta_1\delta$ and/or $\alpha_4\beta_3\delta$ receptors contribute to tonic inhibition in these cells as well, at least in rats. The differential amplitudes of Thio-THIP-induced currents in the 15 VBT neurons could potentially arise from differential expression of the three $\alpha_4\beta\delta$ subtypes in the cells. In line with this, the correlation between basal activity levels and Thio-THIP-induced current amplitudes in these neurons could be a reflection of the higher GABA sensitivities exhibited by $\alpha_4\beta_1\delta$ and $\alpha_4\beta_3\delta$ compared with $\alpha_4\beta_2\delta$ in the oocytes (Figs. 2*D* and 7*G*).

The negligible effects of 100 μM Thio-THIP at synaptic currents in rat striatal MSNs and VBT cells concur with its properties at recombinant $\alpha_{1,2,3}\beta_{2,3}\gamma_2$ receptors (Figs. 3 and 8). Interestingly, the significantly reduced peak amplitudes of mIPSCs recorded from DGGCs in the presence of the compound seem to be attributable to δ-containing receptors (Fig. 8). Since 100 μM Thio-THIP is not expected to affect $\alpha_4\beta_2\delta$ receptors substantially, we speculate that the effect arises from $\alpha_4\beta_{1/3}\delta$ receptors expressed analogously to the proposed perisynaptic $\alpha_4\beta\delta$ receptors in mouse DGCCs (Wei et al., 2003). Occupancy of these receptors by Thio-THIP would counteract the effects of synaptically released GABA, and conversely agonist binding to the receptors would not trigger measurable tonic currents, presumably due to their small magnitude evoked from a distal localization (Soltesz et al., 1995). Finally, as for the concern whether the functionality determined for Thio-THIP at $\alpha_4\beta\delta$ complexes assembled in oocytes is truly representative of its properties at the native receptors, the robust currents induced by the compound in VBT neurons and its effect on mIPSCs in DGCCs certainly suggest that at least some $\alpha_4\beta_{1/3}\delta$ receptors are targeted by the compound, just as its inability to induce currents through the extrasynaptic $GABA_A$Rs in the DGGCs seems to concur with its negligible activity at the recombinant $\alpha_4\beta_2\delta$ receptors.

Thio-THIP: a novel pharmacological tool for explorations of $\alpha_4\beta\delta$ $GABA_A$Rs

In conclusion, we propose that Thio-THIP could be a valuable addition to the rather limited selection of β-isoform-selective $GABA_AR$ ligands currently available. Whereas β-selectivity in previously published ligands has come in the form of β_2/β_3- or β_1-selectivity (Wafford et al., 1994; Belelli et al., 1997; Hill-Venning et al., 1997; Halliwell et al., 1999; Thompson et al., 2004; Absalom et al., 2012), Thio-THIP is to our knowledge the first $GABA_AR$ ligand exhibiting pronounced β_1/β_3-over-β_2-selectivity and thus being able to differentiate between β_2- and β_3-containing subtypes, at least when it comes to $\alpha_4\beta\delta$ receptors. Although Thio-THIP admittedly has not been characterized functionally at all physiologically relevant $GABA_AR$ subtypes, the present data suggest that Thio-THIP (100 μM) will act fairly selectively at $\alpha_4\beta_{1,3}\delta$ and $\alpha_6\beta\delta$ receptors; thus, the compound would be expected to be selective for $\alpha_4\beta_{1,3}\delta$ receptors in most CNS regions, except for cerebellum. Also, in this respect, Thio-THIP differs from the previously published allosteric modulators, which target a wide range of β_2/β_3- or β_1-containing $GABA_AR$ subtypes. On the other hand, the use of Thio-THIP in combination with one of these modulators or in transgenic mice could be an attractive approach to delineate the exact compositions of native $\alpha_4\beta\delta$ receptors, although such an endeavor potentially could face another level of complexity in the form of the putative assembly of "mixed" $\alpha_4\beta\delta$ receptors ($\alpha_4\beta_1\beta_2\delta$, $\alpha_4\beta_1\beta_3\delta$, $\alpha_4\beta_2\beta_3\delta$ or even $\alpha_4\beta_1\beta_2\beta_3\delta$) *in vivo*. Finally, perhaps the most interesting perspective arising from this study is the ability of an β-isoform-selective $\alpha_4\beta\delta$ agonist to affect tonic inhibition in some CNS regions but not in others. Although its moderate potency makes Thio-THIP an unlikely therapeutic candidate, it would nevertheless be interesting to explore whether the discrete modulation of tonic GABAergic signaling in specific brain regions exerted by it could hold some therapeutic advantages compared with drugs acting nonselectively at $\alpha_4\beta\delta$ receptors, such as its close structural analog THIP.

References

Absalom N, Eghorn LF, Villumsen IS, Karim N, Bay T, Olsen JV, Knudsen GM, Bräuner-Osborne H, Frølund B, Clausen RP, Chebib M, Wellendorph P (2012) α4βδ $GABA_A$ receptors are high-affinity targets for γ-hydroxybutyric acid (GHB). Proc Natl Acad Sci U S A 109:13404–13409. CrossRef Medline

Anstee QM, Knapp S, Maguire EP, Hosie AM, Thomas P, Mortensen M, Bhome R, Martinez A, Walker SE, Dixon CI, Ruparelia K, Montagnese S, Kuo YT, Herlihy A, Bell JD, Robinson I, Guerrini I, McQuillin A, Fisher EM, Ungless MA, et al. (2013) Mutations in the *Gabrb1* gene promote alcohol consumption through increased tonic inhibition. Nat Commun 4:2816. CrossRef Medline

Atack JR (2011a) $GABA_A$ receptor subtype-selective modulators: II. α5-Selective inverse agonists for cognition enhancement. Curr Top Med Chem 11:1203–1214. CrossRef Medline

Atack JR (2011b) $GABA_A$ receptor subtype-selective modulators: I. α2/α3-selective agonists as non-sedating anxiolytics. Curr Top Med Chem 11:1176–1202. CrossRef Medline

Barrera NP, Betts J, You H, Henderson RM, Martin IL, Dunn SM, Edwardson JM (2008) Atomic force microscopy reveals the stoichiometry and subunit arrangement of the α4β3δ $GABA_A$ receptor. Mol Pharmacol 73:960–967. CrossRef Medline

Baur R, Kaur KH, Sigel E (2009) Structure of $\alpha6\beta3\delta$ $GABA_A$ receptors and their lack of ethanol sensitivity. J Neurochem 111:1172–1181. CrossRef Medline

Belelli D, Lambert JJ, Peters JA, Wafford K, Whiting PJ (1997) The interaction of the general anesthetic etomidate with the γ-aminobutyric acid type A receptor is influenced by a single amino acid. Proc Natl Acad Sci U S A 94:11031–11036. CrossRef Medline

Belelli D, Peden DR, Rosahl TW, Wafford KA, Lambert JJ (2005) Extrasynaptic $GABA_A$ receptors of thalamocortical neurons: a molecular target for hypnotics. J Neurosci 25:11513–11520. CrossRef Medline

Belelli D, Harrison NL, Maguire J, Macdonald RL, Walker MC, Cope DW (2009) Extrasynaptic $GABA_A$ receptors: form, pharmacology, and function. J Neurosci 29:12757–12763. CrossRef Medline

Borghese CM, Stórustovu S, Ebert B, Herd MB, Belelli D, Lambert JJ, Marshall G, Wafford KA, Harris RA (2006) The δ subunit of γ-aminobutyric acid type A receptors does not confer sensitivity to low concentrations of ethanol. J Pharmacol Exp Ther 316:1360–1368. CrossRef Medline

Bräuner-Osborne H, Krogsgaard-Larsen P (1999) Functional pharmacology of cloned heterodimeric $GABA_B$ receptors expressed in mammalian cells. Br J Pharmacol 128:1370–1374. CrossRef Medline

Brehm L, Ebert B, Kristiansen U, Wafford KA, Kemp JA, Krogsgaard-Larsen P (1997) Structure and pharmacology of 4,5,6,7-tetrahydroisothiazolo[5,4-c]pyridin-3-ol (Thio-THIP), an agonist/antagonist at $GABA_A$ receptors. Eur J Med Chem 32:357–363. CrossRef

Brickley SG, Mody I (2012) Extrasynaptic $GABA_A$ receptors: their function in the CNS and implications for disease. Neuron 73:23–34. CrossRef Medline

Brickley SG, Revilla V, Cull-Candy SG, Wisden W, Farrant M (2001) Adaptive regulation of neuronal excitability by a voltage-independent potassium conductance. Nature 409:88–92. CrossRef Medline

Brown N, Kerby J, Bonnert TP, Whiting PJ, Wafford KA (2002) Pharmacological characterization of a novel cell line expressing human $\alpha_4\beta_3\delta$ $GABA_A$ receptors. Br J Pharmacol 136:965–974. CrossRef Medline

Chandra D, Jia F, Liang J, Peng Z, Suryanarayanan A, Werner DF, Spigelman I, Houser CR, Olsen RW, Harrison NL, Homanics GE (2006) $GABA_A$ receptor α_4 subunits mediate extrasynaptic inhibition in thalamus and dentate gyrus and the action of gaboxadol. Proc Natl Acad Sci U S A 103:15230–15235. CrossRef Medline

Christiansen B, Kvist T, Jensen AA, Bräuner-Osborne H (2008) The human γ-aminobutyric acid transporter GAT-2: from cloning to high throughput screening In: Innovative drug development for headache disorders: Frontiers in headache research (Olesen J, Ramadan N, eds), pp 3–15. Oxford, United Kingdom: Oxford UP.

Conklin BR, Farfel Z, Lustig KD, Julius D, Bourne HR (1993) Substitution of three amino acids switches receptor specificity of $G_q\alpha$ to that of $G_i\alpha$. Nature 363:274–276. CrossRef Medline

Connolly CN, Wooltorton JR, Smart TG, Moss SJ (1996) Subcellular localization of γ-aminobutyric acid type A receptors is determined by receptor β subunits. Proc Natl Acad Sci U S A 93:9899–9904. CrossRef Medline

Duthey B, Caudron S, Perroy J, Bettler B, Fagni L, Pin JP, Prézeau L (2002) A single subunit (GB2) is required for G-protein activation by the heterodimeric $GABA_B$ receptor. J Biol Chem 277:3236–3241. CrossRef Medline

Eaton M, Bracamontes J, Shu HJ, Li P, Mennerick SJ, Steinbach JH, Akk G (2014) $GABA_A$ α4, β2 and δ subunits assemble to produce more than one functionally distinct receptor type. Mol Pharmacol 86:647–656. CrossRef Medline

Ebert B, Wafford KA, Deacon S (2006) Treating insomnia: current and investigational pharmacological approaches. Pharmacol Ther 112:612–629. CrossRef Medline

Eiselé JL, Bertrand S, Galzi JL, Devillers-Thiéry A, Changeux JP, Bertrand D (1993) Chimaeric nicotinic-serotonergic receptor combines distinct ligand binding and channel specificities. Nature 366:479–483. CrossRef Medline

Eyre MD, Renzi M, Farrant M, Nusser Z (2012) Setting the time course of inhibitory synaptic currents by mixing multiple $GABA_A$ receptor α subunit isoforms. J Neurosci 32:5853–5867. CrossRef Medline

Farrant M, Nusser Z (2005) Variations on an inhibitory theme: phasic and tonic activation of $GABA_A$ receptors. Nat Rev Neurosci 6:215–229. CrossRef Medline

Flores-Hernandez J, Hernandez S, Snyder GL, Yan Z, Fienberg AA, Moss SJ, Greengard P, Surmeier DJ (2000) D_1 dopamine receptor activation reduces $GABA_A$ receptor currents in neostriatal neurons through a PKA/DARPP-32/PP1 signaling cascade. J Neurophysiol 83:2996–3004. Medline

Glykys J, Peng Z, Chandra D, Homanics GE, Houser CR, Mody I (2007) A new naturally occurring $GABA_A$ receptor subunit partnership with high sensitivity to ethanol. Nat Neurosci 10:40–48. CrossRef Medline

Halliwell RF, Thomas P, Patten D, James CH, Martinez-Torres A, Miledi R, Smart TG (1999) Subunit-selective modulation of $GABA_A$ receptors by the non-steroidal anti-inflammatory agent, mefenamic acid. Eur J Neurosci 11:2897–2905. CrossRef Medline

Herd MB, Haythornthwaite AR, Rosahl TW, Wafford KA, Homanics GE, Lambert JJ, Belelli D (2008) The expression of $GABA_A$ β subunit isoforms in synaptic and extrasynaptic receptor populations of mouse dentate gyrus granule cells. J Physiol 586:989–1004. Medline

Herd MB, Foister N, Chandra D, Peden DR, Homanics GE, Brown VJ, Balfour DJ, Lambert JJ, Belelli D (2009) Inhibition of thalamic excitability by 4,5,6,7-tetrahydroisoxazolo[4,5-c]pyridine-3-ol: a selective role for δ-$GABA_A$ receptors. Eur J Neurosci 29:1177–1187. CrossRef Medline

Hermit MB, Greenwood JR, Nielsen B, Bunch L, Jørgensen CG, Vestergaard HT, Stensbøl TB, Sanchez C, Krogsgaard-Larsen P, Madsen U, Bräuner-Osborne H (2004) Ibotenic acid and thioibotenic acid: a remarkable difference in activity at group III metabotropic glutamate receptors. Eur J Pharmacol 486:241–250. CrossRef Medline

Hill-Venning C, Belelli D, Peters JA, Lambert JJ (1997) Subunit-dependent interaction of the general anaesthetic etomidate with the γ-aminobutyric acid type A receptor. Br J Pharmacol 120:749–756. CrossRef Medline

Hoestgaard-Jensen K, Dalby NO, Wolinsky TD, Murphey C, Jones KA, Rottländer M, Frederiksen K, Watson WP, Jensen K, Ebert B (2010) Pharmacological characterization of a novel positive modulator at $\alpha4\beta3\delta$-containing extrasynaptic $GABA_A$ receptors. Neuropharmacology 58:702–711. CrossRef Medline

Hoestgaard-Jensen K, O'Connor RM, Dalby NO, Simonsen C, Finger BC, Golubeva A, Hammer H, Bergmann ML, Kristiansen U, Krogsgaard-Larsen P, Bräuner-Osborne H, Ebert B, Frølund B, Cryan JF, Jensen AA (2013) The orthosteric $GABA_A$ receptor ligand 5-(4-piperidyl)-3-isothiazolol (Thio-4-PIOL) displays distinctly different functional properties at synaptic and extrasynaptic receptors. Br J Pharmacol 170:919–932. CrossRef Medline

Hörtnagl H, Tasan RO, Wieselthaler A, Kirchmair E, Sieghart W, Sperk G (2013) Patterns of mRNA and protein expression for 12 $GABA_A$ receptor subunits in the mouse brain. Neuroscience 236:345–372. CrossRef Medline

Horton RM, Hunt HD, Ho SN, Pullen JK, Pease LR (1989) Engineering hybrid genes without the use of restriction enzymes: gene splicing by overlap extension. Gene 77:61–68. CrossRef Medline

Houston CM, He Q, Smart TG (2009) CaMKII phosphorylation of the $GABA_A$ receptor: receptor subtype- and synapse-specific modulation. J Physiol 587:2115–2125. CrossRef Medline

Janssen MJ, Ade KK, Fu Z, Vicini S (2009) Dopamine modulation of GABA tonic conductance in striatal output neurons. J Neurosci 29:5116–5126. CrossRef Medline

Jensen AA, Bergmann ML, Sander T, Balle T (2010) Ginkgolide X is a potent antagonist of anionic Cys-loop receptors with a unique selectivity profile at glycine receptors. J Biol Chem 285:10141–10153. CrossRef Medline

Jia F, Pignataro L, Schofield CM, Yue M, Harrison NL, Goldstein PA (2005) An extrasynaptic $GABA_A$ receptor mediates tonic inhibition in thalamic VB neurons. J Neurophysiol 94:4491–4501. CrossRef Medline

Jones A, Korpi ER, McKernan RM, Pelz R, Nusser Z, Mäkelä R, Mellor JR, Pollard S, Bahn S, Stephenson FA, Randall AD, Sieghart W, Somogyi P, Smith AJ, Wisden W (1997) Ligand-gated ion channel subunit partnerships: $GABA_A$ receptor α6 subunit gene inactivation inhibits δ subunit expression. J Neurosci 17:1350–1362. Medline

Karim N, Wellendorph P, Absalom N, Bang LH, Jensen ML, Hansen MM, Lee HJ, Johnston GA, Hanrahan JR, Chebib M (2012) Low nanomolar GABA effects at extrasynaptic $\alpha4\beta1/\beta3\delta$ $GABA_A$ receptor subtypes indicate a different binding mode for GABA at these receptors. Biochem Pharmacol 84:549–557. CrossRef Medline

Karim N, Wellendorph P, Absalom N, Johnston GA, Hanrahan JR, Chebib M (2013) Potency of GABA at human recombinant $GABA_A$ receptors expressed in *Xenopus* oocytes: a mini review. Amino Acids 44:1139–1149. CrossRef Medline

Kaur KH, Baur R, Sigel E (2009) Unanticipated structural and functional properties of δ-subunit-containing $GABA_A$ receptors. J Biol Chem 284:7889–7896. CrossRef Medline

Kittler JT, Moss SJ (2003) Modulation of $GABA_A$ receptor activity by phos-

phorylation and receptor trafficking: implications for the efficacy of synaptic inhibition. Curr Opin Neurobiol 13:314–347. CrossRef Medline

Krehan D, Frølund B, Ebert B, Nielsen B, Krogsgaard-Larsen P, Johnston GA, Chebib M (2003) Aza-THIP and related analogues of THIP as $GABA_C$ antagonists. Bioorg Med Chem 11:4891–4896. CrossRef Medline

Krishek BJ, Moss SJ, Smart TG (1996) Homomeric β1 γ-aminobutyric acid A receptor-ion channels: evaluation of pharmacological and physiological properties. Mol Pharmacol 49:494–504. Medline

Krogsgaard-Larsen P, Johnston GA, Lodge D, Curtis DR (1977) A new class of GABA agonist. Nature 268:53–55. CrossRef Medline

Krogsgaard-Larsen P, Mikkelsen H, Jacobsen P, Falch E, Curtis DR, Peet MJ, Leah JD (1983) 4,5,6,7-Tetrahydroisothiazolo[5,4-c]pyridin-3-ol and related analogues of THIP: synthesis and biological activity. J Med Chem 26:895–900. CrossRef Medline

Kvist T, Christiansen B, Jensen AA, Bräuner-Osborne H (2009) The four human γ-aminobutyric acid (GABA) transporters: pharmacological characterization and validation of a highly efficient screening assay. Comb Chem High Throughput Screen 12:241–249. CrossRef Medline

Laurie DJ, Wisden W, Seeburg PH (1992) The distribution of thirteen $GABA_A$ receptor subunit mRNAs in the rat brain: III. Embryonic and postnatal development. J Neurosci 12:4151–4172. Medline

Lovick TA, Griffiths JL, Dunn SM, Martin IL (2005) Changes in $GABA_A$ receptor subunit expression in the midbrain during the oestrous cycle in Wistar rats. Neuroscience 131:397–405. CrossRef Medline

Luo R, Partridge JG, Vicini S (2013) Distinct roles of synaptic and extrasynaptic $GABA_A$ receptors in striatal inhibition dynamics. Front Neural Circuits 7:186. CrossRef Medline

Marowsky A, Rudolph U, Fritschy JM, Arand M (2012) Tonic inhibition in principal cells of the amygdala: a central role for α3 subunit-containing $GABA_A$ receptors. J Neurosci 32:8611–8619. CrossRef Medline

Matzen L, Engesgaard A, Ebert B, Didriksen M, Frølund B, Krogsgaard-Larsen P, Jaroszewski JW (1997) AMPA receptor agonists: synthesis, protolytic properties, and pharmacology of 3-isothiazolol bioisosteres of glutamic acid. J Med Chem 40:520–527. CrossRef Medline

Meera P, Olsen RW, Otis TS, Wallner M (2009) Etomidate, propofol and the neurosteroid THDOC increase the GABA efficacy of recombinant $\alpha4\beta3\delta$ and $\alpha4\beta3$ $GABA_A$ receptors expressed in HEK cells. Neuropharmacology 56:155–160. CrossRef Medline

Meera P, Wallner M, Otis TS (2011) Molecular basis for the high THIP/gaboxadol sensitivity of extrasynaptic $GABA_A$ receptors. J Neurophysiol 106:2057–2064. CrossRef Medline

Milenkovic I, Vasiljevic M, Maurer D, Hoger H, Klausberger T, Sieghart W (2013) The parvalbumin-positive interneurons in the mouse dentate gyrus express GABA receptor subunits α1, β2, and δ along their extrasynaptic cell membrane. Neuroscience 254:80–96. CrossRef Medline

Mortensen M, Smart TG (2006) Extrasynaptic αβ subunit $GABA_A$ receptors on rat hippocampal pyramidal neurons. J Physiol 577:841–856. CrossRef Medline

Mortensen M, Kristiansen U, Ebert B, Frølund B, Krogsgaard-Larsen P, Smart TG (2004) Activation of single heteromeric $GABA_A$ receptor ion channels by full and partial agonists. J Physiol 557:389–413. CrossRef Medline

Mortensen M, Ebert B, Wafford K, Smart TG (2010) Distinct activities of GABA agonists at synaptic- and extrasynaptic-type $GABA_A$ receptors. J Physiol 588:1251–1268. CrossRef Medline

Mortensen M, Patel B, Smart TG (2011) GABA potency at $GABA_A$ receptors found in synaptic and extrasynaptic zones. Front Cell Neurosci 6:1. CrossRef Medline

Nusser Z, Mody I (2002) Selective modulation of tonic and phasic inhibitions in dentate gyrus granule cells. J Neurophysiol 87:2624–2628. Medline

Olsen RW, Sieghart W (2008) International Union of Pharmacology. LXX. Subtypes of γ-aminobutyric $acid_A$ receptors: classification on the basis of subunit composition, pharmacology, and function. Update. Pharmacol Rev 60:243–260. CrossRef Medline

Patel B, Mortensen M, Smart TG (2014) Stoichiometry of δ subunit containing $GABA_A$ receptors. Br J Pharmacol 171:985–994. CrossRef Medline

Pirker S, Schwarzer C, Wieselthaler A, Sieghart W, Sperk G (2000) $GABA_A$ receptors: immunocytochemical distribution of 13 subunits in the adult rat brain. Neuroscience 101:815–850. CrossRef Medline

Reynolds DS, Rosahl TW, Cirone J, O'Meara GF, Haythornthwaite A, Newman RJ, Myers J, Sur C, Howell O, Rutter AR, Atack J, Macaulay AJ, Hadingham KL, Hutson PH, Belelli D, Lambert JJ, Dawson GR, McKernan R, Whiting PJ, Wafford KA (2003) Sedation and anesthesia mediated by distinct $GABA_A$ receptor isoforms. J Neurosci 23:8608–8617. Medline

Rudolph U, Knoflach F (2011) Beyond classical benzodiazepines: novel therapeutic potential of $GABA_A$ receptor subtypes. Nat Rev Drug Discov 10:685–697. CrossRef Medline

Sanna E, Garau F, Harris RA (1995) Novel properties of homomeric β1 γ-aminobutyric acid type A receptors: actions of the anesthetics propofol and pentobarbital. Mol Pharmacol 47:213–217. Medline

Shu HJ, Bracamontes J, Taylor A, Wu K, Eaton MM, Akk G, Manion B, Evers AS, Krishnan K, Covey DF, Zorumski CF, Steinbach JH, Mennerick S (2012) Characteristics of concatemeric $GABA_A$ receptors containing α4/δ subunits expressed in *Xenopus* oocytes. Br J Pharmacol 165:2228–2243. CrossRef Medline

Sieghart W (2006) Structure, pharmacology, and function of $GABA_A$ receptor subtypes. Adv Pharmacol 54:231–263. CrossRef Medline

Simeone TA, Wilcox KS, White HS (2011) Topiramate modulation of β_1- and β_3-homomeric $GABA_A$ receptors. Pharmacol Res 64:44–52. CrossRef Medline

Soltesz I, Smetters DK, Mody I (1995) Tonic inhibition originates from synapses close to the soma. Neuron 14:1273–1283. CrossRef Medline

Stell BM, Brickley SG, Tang CY, Farrant M, Mody I (2003) Neuroactive steroids reduce neuronal excitability by selectively enhancing tonic inhibition mediated by δ subunit-containing $GABA_A$ receptors. Proc Natl Acad Sci U S A 100:14439–14444. CrossRef Medline

Stórustovu SI, Ebert B (2006) Pharmacological characterization of agonists at δ-containing $GABA_A$ receptors: functional selectivity for extrasynaptic receptors is dependent on the absence of γ2. J Pharmacol Exp Ther 316:1351–1359. CrossRef Medline

Sur C, Farrar SJ, Kerby J, Whiting PJ, Atack JR, McKernan RM (1999) Preferential coassembly of α4 and δ subunits of the γ-aminobutyric $acid_A$ receptor in rat thalamus. Mol Pharmacol 56:110–115. CrossRef Medline

Taylor PM, Thomas P, Gorrie GH, Connolly CN, Smart TG, Moss SJ (1999) Identification of amino acid residues within $GABA_A$ receptor β subunits that mediate both homomeric and heteromeric receptor expression. J Neurosci 19:6360–6371. Medline

Thompson SA, Wheat L, Brown NA, Wingrove PB, Pillai GV, Whiting PJ, Adkins C, Woodward CH, Smith AJ, Simpson PB, Collins I, Wafford KA (2004) Salicylidene salicylhydrazide, a selective inhibitor of β1-containing $GABA_A$ receptors. Br J Pharmacol 142:97–106. CrossRef Medline

Vien J, Duke RK, Mewett KN, Johnston GA, Shingai R, Chebib M (2002) trans-4-Amino-2-methylbut-2-enoic acid (2-MeTACA) and (+/-)-trans-2-aminomethylcyclopropanecarboxylic acid ((+/-)-TAMP) can differentiate rat ρ3 from human ρ1 and ρ2 recombinant $GABA_C$ receptors. Br J Pharmacol 135:883–890. CrossRef Medline

Wafford KA, Bain CJ, Quirk K, McKernan RM, Wingrove PB, Whiting PJ, Kemp JA (1994) A novel allosteric modulatory site on the $GABA_A$ receptor β subunit. Neuron 12:775–782. CrossRef Medline

Wafford KA, van Niel MB, Ma QP, Horridge E, Herd MB, Peden DR, Belelli D, Lambert JJ (2009) Novel compounds selectively enhance δ subunit containing $GABA_A$ receptors and increase tonic currents in thalamus. Neuropharmacology 56:182–189. CrossRef Medline

Wei W, Zhang N, Peng Z, Houser CR, Mody I (2003) Perisynaptic localization of δ subunit-containing $GABA_A$ receptors and their activation by GABA spillover in the mouse dentate gyrus. J Neurosci 23:10650–10661. Medline

Whiting PJ (2003) GABA-A receptor subtypes in the brain: a paradigm for CNS drug discovery? Drug Discov Today 8:445–450. CrossRef Medline

Wisden W, Laurie DJ, Monyer H, Seeburg PH (1992) The distribution of 13 $GABA_A$ receptor subunit mRNAs in the rat brain: I. Telencephalon, diencephalon, mesencephalon. J Neurosci 12:1040–1062. Medline

Woodward RM, Polenzani L, Miledi R (1993) Characterization of bicuculline/baclofen-insensitive (ρ-like) γ-aminobutyric acid receptors expressed in *Xenopus* oocytes: II. Pharmacology of γ-aminobutyric $acid_A$ and γ-aminobutyric $acid_B$ receptor agonists and antagonists. Mol Pharmacol 43:609–625. Medline

Zhang N, Wei W, Mody I, Houser CR (2007) Altered localization of $GABA_A$ receptor subunits on dentate granule cell dendrites influences tonic and phasic inhibition in a mouse model of epilepsy. J Neurosci 27:7520–7531. CrossRef Medline